ADDIS ABABA UNIVERSITY

COLLEGE OF NATURAL AND COMPUTATIONAL SCIENCES

SCHOOL OF EARTH SCIENCES

GIS-Based Landslide Susceptibility Mapping in Wuchale area, South Wollo Zone, Northern Ethiopia

A Thesis submitted to the School of Earth Sciences, Addis Ababa University, in partial fulfillment of the requirements for the Degree of Master of Science, in Geological Engineering (Environmental Geology and Geohazards)

Haile Alemu Chekole

June, 2024

Addis Ababa, Ethiopia

Addis Ababa University

School of Earth Sciences

GIS-Based Landslide Susceptibility Mapping in Wuchale area, South Wollo Zone, Northern Ethiopia

Haile Alemu Chekole

ID.No: GSR/7389/15

Advisor: Dr.Trufat Hailemariam

Co-advisor: Dr.Tibebu Kassawmar

A Thesis submitted to the School of Earth Sciences, Addis Ababa University, in partial fulfillment of the requirements for the Degree of Master of Science, in Geological Engineering (Environmental Geology and Geohazards)

June, 2024

Addis Ababa, Ethiopia

Declaration page

I formally affirm that the thesis titled: **GIS-Based Landslide Susceptibility Mapping in Wuchale area, South Wollo Zone, Northern Ethiopia** is my original work, conducted under the guidance of my thesis mentors, and that I have acknowledged all sources used in this thesis.

Haile Alemu Chekole		
Name	Signature	Date

Signature page

This is to confirm that the thesis titled **'GIS–Based Landslide Susceptibility Mapping in Wuchale area, South Wollo Zone, Northern Ethiopia'** prepared by Haile Alemu and submitted in partial fulfillment of the requirements for the Degree of Master of Science in Environmental Geology and Geohazards, adheres to the University's regulations and meets the accepted standards for originality and quality.

This thesis has been examined and approved by the following members of the thesis committee:

Advisor:

Dr. Trufat Hailemariam

Name	Signature	Date

Co-advisor:

Dr. Tibebu Kassawmar

Name	Signature	Date

Internal examiner:

Dr. Binyam Tesfaw

Name	Signature	Date

External examiner:

Dr. Tesfaye Asresahagne

Name	Signature	Date

Chair of School or Graduate Program Coordinator

Abstract

This study was conducted in the Wuchale area in the Amhara regional state of the South Wollo Zone, northern Ethiopia. The study aims to evaluate and map landslide susceptibility in the area. A bivariate statistical information value and frequency ratio models were employed to achieve this objective. Six factor layers responsible for landslide occurrences including slope, aspect, elevation, lithology, LULC, and distance to stream were analyzed. With the aid of GPS devices and Google Earth Image interpretations, 31 landslide inventory points were identified. All the data layers were rasterized with a uniform pixel size of 12.5 m in ArcGIS 10.4, which helps to count the amount of entire pixels and landslide pixels uniformly in the area. The frequency ratio and information value models were applied to 70% (22) of the landslide inventory points to determine the relative significance of each factor class. The weights of each factor class were summed to generate a final landslide susceptibility map using a GIS raster calculator. Using natural breaks interval (Jenks), the research region was categorized into five (5) susceptibility classes: very low, low, moderate, high, and very high considering the landslide susceptibility index ranges. The FR model results indicate that 9 km^2 (9%) of the area is covered by very high susceptibility, 11 km^2 (11%) by high susceptibility, 17 km^2 (17%) by moderate susceptibility, 23 km^2 (23%) by low susceptibility, and 40 km^2 (40) by very low susceptibility. Similarly, the IV model shows 18 km^2 (18%) with very high susceptibility, 12 km^2 (12%) with high susceptibility, 17 km^2 (17%) with moderate susceptibility, 18 km^2 (18%) with low susceptibility, and 35 km^2 (35) with very low susceptibility. Validation of the susceptibility map was conducted using 30% (9) of landslide inventory points that were not used in the model–building, yielding area under the curve (AUC) values of 0.78 and 0.828 for the frequency ratio model's success and prediction rates, respectively. The information value model achieved success and prediction rates of 0.786 and 0.83, respectively. These validation results demonstrate satisfactory agreement between the landslide susceptibility map and existing landslides.

Keywords: Frequency ratio, information value, landslide, landslide susceptibility, validation, Wuchale.

Acknowledgments

To begin with, I want to convey my sincere gratitude to Wollo University for providing me with full sponsorship, which has been instrumental in supporting my academic journey and research endeavors.

I am deeply grateful to my mentor, Dr.Trufat Hailemariam, and co-mentor, Dr.Tibebu Kassawmar, for their guidance, expertise, and reliable support throughout this research work. Their mentorship and constructive feedback have been invaluable in shaping this thesis and enhancing my academic and research capabilities.

I am also grateful to Addis Ababa University for its significant contribution to my MSc program, the development of my academic growth, and enabling me to pursue advanced studies in my field.

Special appreciation goes to the Space Science and Geospatial Institute of Ethiopia, GSE, and the Ethiopian Meteorological Institute for providing valuable secondary data essential for conducting this research. Their support and resources have greatly facilitated the accomplishment of this study.

I extend my heartfelt thanks to Ato Tesfaye Melaku, Head of the Ambasel Woreda Agriculture Office's Disaster Response and Early Warning Team. His assistance and cooperation have been invaluable in gathering essential information and insights for this research.

Lastly, I would like to extend my heartfelt thanks to my friends and families for their continuous motivation, inspiration, and assistance during this challenging and rewarding journey.

Haile Alemu Chekole

Table of contents

Contents page

List of Figures

List of Tables

Acronyms

AHP	Analytic Hierarchy Process
ALOS	Advanced Land Observing Satellite
AUC	Area under the Curve
CFB	Continental Flood Basalt
DEM	Digital Elevation Model
EARV	East African Rift Valley
FAO	Food and Agriculture Organization
FR	Frequency Ratio
GIS	Geographic Information System
GSE	Geological Survey of Ethiopia
IV	Information Value
LHZ	Landslide Hazard Zonation
LSI	Landslide Susceptibility Index
LULC	Land Use Land Cover
MER	Main Ethiopian Rift
NDVI	Normalized Difference Vegetation Index
PALSAR	Phased Array L-band Synthetic Aperture Radar
ROC	Receiver Operator Curve
RS	Remote Sensing
SSGI	Space Science and Geospatial Institute

CHAPTER I

INTRODUCTION

1.2 Background

The word landslide has several definitions depending on different disciplines. Landslides are an embracing term employed to explain the downward motion of slope materials (soils and rocks) due to the influence of gravity, causing modifications to the morphology of the surface of the earth (Highland & Bobrowsky, 2008). It is also defined as geomorphic incidents with a sudden or slowly downward movement of soil or rocks in a sloppy topography (Singhroy, 1995). It is among the world's most severe natural processes, these cause deaths, vast damage to infrastructures, and disruption of a multitude of resources (Kanungo et al., 2009; Sarkar & Kanungo, 2004). In addition to these casualties, landslide has a great influence on our natural environment including changing the aesthetic view of the earth's surface, destroying grasslands and forests, displacing wildlife, and disturbing waterbodies (rivers, lakes, and seas) (Highland & Bobrowsky, 2008).

Wuchale area is situated in rugged terrain in northern Ethiopia. Most of the landslide activities have occurred recently in the area. Residential structures, roads, croplands, and lifeline infrastructure in the area were damaged by frequent landslide events, and residents had to be evacuated from their homes. The area will see an increase in landslides due to human intervention and inherent responsible factors, which will result in infrastructure damage and fatalities.

Therefore, to reduce such a devastating hazard, it is crucial to delineate the hazard-prone area before the hazard affects human life, landscapes, and infrastructure. To delineate an area, various analysis techniques can be applied for various levels of susceptibility (Anbalagan, 1992). This research employed a bivariate statistical frequency ratio and information value models to evaluate and classify the area into different susceptibility classes.

To reduce the extent of the damage and compensate affected societies, landslide susceptibility mapping is a critical technique. Therefore, this research is the first to address an investigation of landslide susceptibilities in the specified area and create an enhanced insight of the likelihood of landslide events for the government and local community.

1.2 Statement of the problem

The study area is located in rugged terrain in northern Ethiopia in the Amhara regional state of the South Wollo Zone. Landslide hazards pose a significant environmental challenge within the study region, impacting essential infrastructure, residential structures, and the landscape. According to the South Wollo Zone Government Communication Affairs report dated 11 December 2022, five hundred and thirty-three (533), families have been displaced due to landslide hazards in the area known as Graar Genda in the Ambasel woreda of the South Wollo Zone. Ato Tesfaye Melaku, Head of the Ambasel Woreda Agriculture Office's Disaster Response and Early Warning Team, reported that 174 houses have been damaged so far, and the natural disasters are increasing daily (https://southwollocommunication.gov.et/News/SinglePost/535).

The area is heavily affected by landslides, but no previous survey has been documented in the area. Hazard zoning, prediction, modeling, and monitoring are crucial to reducing hazards, informing the public and government regarding the likelihood of landslides, and promoting better land use planning practices. Hence, this study aims to determine landslide-prone areas and create landslide susceptibility maps. This will alert the government and local community to the likelihood of landslides in the Wuchale area and suggest better land use planning practices for a safer future.

1.3 Objectives

1.3.1 General objective

The primary objective of this research is to generate a landslide susceptibility map of Wuchale town and its surroundings using a GIS-Based statistical approach.

1.3.2 Specific objectives

The research has the following particular goals:

- To prepare a landslide inventory map of the Wuchale area.
- To determine and assess the potential contributing elements to landslides.
- To assess the relative significance of each casual factor in causing landslides.
- To generate landslide susceptibility maps of the study area.

1.4 Significance of the research

As previously mentioned in section 1.2, the occurrence of landslide hazards in the Wuchale area has led to evacuations of people, damage to houses, and destruction of infrastructure such as roads, electricity lines, and water pipes. This research is the first to address a comprehensive landslide susceptibility investigation in the region, presenting several paramount implications. Firstly, it aids in identifying areas prone to landslide hazards and assists planners in selecting suitable locations for infrastructure development. Moreover, it serves to promote the implementation of best practices in land use planning. Additionally, the information emanating from this research provides valuable insights that can significantly enhance decision-making processes in the specified area. Furthermore, the collected field data and analysis results will be utilized in a data management system for students, the scientific community, and any interested investigators in the particular area.

1.5 Research outcomes

This study conducted in the Wuchale area aimed to assess landslide susceptibility. It involved preparing a detailed landslide inventory map, identifying and evaluating potential factors contributing to landslides, assessing the relative significance of causal factors, and generating a landslide susceptibility map. These outcomes contribute to a better understanding of landslide susceptibility in the study area.

1.6 Thesis organization

This thesis is organized into seven (7) chapters and many subtopics within each chapter.

Chapter One: is concerned with the general introduction of the work which contains background, a statement of the problem, objectives, the significance of the research, research outcome, and the thesis structure itself. All these are well explained in each part of the subtopics within the chapter.

Chapter Two: is concerned with the literature about landslides definition, type, conditioning factors, and techniques for mapping landslide susceptible zones. Each of these is described thoroughly in chapter two within parts of each subtopic. In general, this chapter addresses the review of relevant literature related to the research topic, and discussion of key theories, concepts, and findings.

Chapter Three: focused on the general overview of the study area including location, climate, geology, topography, hydrogeology, failure mechanisms, and extent of damages. Each of these listed here is explained very well in chapter three.

Chapter Four: this chapter presents the description of research designs and approaches, an explanation on method of data collection, and details of data analysis. All the methodology phases were clearly explained in this portion. The particular methodology selected for this research is also presented.

Chapter Five: this is the main important part of the research, in which all the data compiled from archived sources and the field are analyzed and processed. The landslide casual elements like aspect, elevation, slope, lithology, stream distance, and LULC were processed in a GIS environment and overlaid on landslide inventory data. After all the necessary steps were conducted, the FR and IV values were calculated in this chapter. Subsequently, the final landslide susceptibility map was produced.

Chapter Six: the findings obtained in the work have been well explained and presented in this chapter. Figures and tables were used to illustrate key findings of the work. It also contains basic discussions from each topic which are necessary to raise. In the discussion part, the interpretation of results concerning research objectives, analysis of findings in the context of existing literature, and explanation of findings were explained. Validation of the model based on AUC is also performed in this chapter.

Chapter Seven: this is the final chapter which contains the conclusion and recommendation. In this chapter, a summary of key findings was comprehensively explained. Additionally, recommendations for future study are also suggested in this chapter.

CHAPTER II

LITERATURE REVIEW

2.1 Landslides: An Overview

Landslide has several definitions depending on different disciplines. Landslides are an embracing term employed to explain the downward motion of slope materials (soils and rocks) due to the influence of gravity, which alters the surface morphology of the earth (Highland & Bobrowsky, 2008). The slope materials like soil, rocks, synthetic fill, or these materials combined can move in various forms like sliding, toppling, falling, spreading, or flowing (Varnes, 1978). It can happen on any type of surface if certain requirements are met, and it can destroy vegetation, water systems, wildlife, farmlands, and demolished infrastructure (Nikolic, 2015). The hazards emanating from landslides are becoming progressively more common problems, especially in the hilly topography of Ethiopia (Bekele Abebe et al., 2010). This hazard's occurrence is influenced by the relative influence of causative parameters like LULC, slope, aspect, elevation, geology, groundwater, and triggering factors like seismicity, heavy rainfall, and anthropogenic factors (Azemeraw Wubalem, 2020; Raghuvanshi et al., 2014).

Landslides can be grouped based on various criteria, incorporating the sliding plane's geometry, the kind of sliding material, the mode and rate of movement, and other factors (Highland & Bobrowsky, 2008). Accordingly, the most known classification scheme was suggested by Varnes (1984) depending on the style of movement and the kind of slope materials constituent as slides, falls, flows, topples, spreads, and complex movements.

2.2 Landslide causing factors

The combination of geological, geomorphological, and hydrogeological elements, as well as seismicity, heavy rainfall, and anthropogenic factors can result in landslides. These factors can significantly impact the formation of landslides in specific areas, depending on their relative contribution. The factors causing slope instability can be categorized into inherent and extrinsic factors (Raghuvanshi et al., 2014).

2.2.1 Intrinsic factors

Internal parameters like slope geometry, weak zones, slope material, groundwater, and LULC can be thought of as the inherent influencing elements that affect slope stability (Highland & Bobrowsky, 2008; Raghuvanshi et al., 2014).

2.2.1.1 Slope material

In a landslide, the slope materials involve rocks (which are hard, strong, and intact before being moved from their original place), soils (any loose, unconsolidated material that is either transported or residual), or a combination of both (Varnes, 1978). The type and composition of lithology have a major impact on slope stability (Li et al., 2021). Lithological data are the principal source in the zonation of landslide hazards, and they are generally attained from the existing geological map and field survey. The geological map of Ethiopia is prepared in 1:250, 0000, and 1:2,000,000 scale e.g. (Mengesha Tefera et al., 1996; Tesfaye Demissie et al., 2010). Such uneven data might not be suitable for landslide hazard analysis when the lithological unit contribution is dominant in the area (Henriques et al., 2015). To obtain good quality lithological data of the area, we must have to prepare a detailed geological map at a large scale.

2.2.1.2 Slope geometry

Slope geometry signifies to the characteristics of a slope, including its slope aspect, elevation, and curvature, which includes its steepness and relief (Raghuvanshi et al., 2014). DEM data from the ASTER satellite can be utilized to determine slope, aspect, elevation, and curvature (Tilahun Hamza & Raghuvanshi, 2017). A steeper slope is more vulnerable to deformation and failure due to the increased shear stress at its base. Aspect indirectly impacts the formation of landslides because the amount of solar radiation received by different slope features of a surface influences vegetation cover, evaporation, and erosion (Li et al., 2021).

2.2.1.3 Structural discontinuity

The pre-existing weak zones, such as faults, joints, foliations, veins, fissures, cleavage, and bedding planes significantly impact the slope's stability. These weak zones appear to be the preferred location for slope failure. However, in contrast, the failure process of slopes is complex and can arise from an intricate interaction between discontinuities and rock matrix, suggesting failure is not restricted to pre-existing discontinuities (Sun et al., 2022). Besides the existence of

discontinuities, its orientation, spacing, persistence, surface properties, and infilling materials have a great influence on the slope's stability (Duncan & Norman, 1996).

2.2.1.4 Condition of groundwater

There are many types of water in the world based on their composition, source, and location. Among these, groundwater is the one that provides a lot of drinking water for us. Apart from its benefits, it has a great impact on the incidence, development, and progression of slope instability (Zhao et al., 2016). Infiltration from intense rainfall or other sources can influence the slope's stability by decreasing the shear resistance of the material and enhancing the factors that promote instability (Picarelli et al., 2012). Additionally, the weak zones below the water table can store and easily transmit water within them; consequently, the water fills the pore spaces and exerts pore water pressure, which tends to strengthen the shear stress and reduce the shear resistance of the material (Picarelli et al., 2012).

2.2.1.5 Land use–land cover

"Land cover" is a word that indicates all the bio-physical components of the earth, comprising both natural features and surfaces that human actions have modified. Conversely, land use refers to human activities that involve the modification and utilization of the land surface and its components for social and economic purposes (Herold et al., 2006). The likelihood of a landslide has been progressively influenced by anthropogenic activities; thus, change in LULC must be considered in a landslide hazard investigation (Pacheco Quevedo et al., 2023). Changes in LULC may influence the landslide's occurrence by altering the geological conditions (Chen et al., 2019). Through its roots, vegetation can enhance slope stability and soil erosion because the roots uptake more water and bind the soil together, thus reducing the water content in the soil (Löbmann et al., 2020). On the contrary, human activities like mining, deforestation, improper farming, road construction, and buildings can reduce the slope's stability (Chen et al., 2019).

2.2.2 External parameters

These are occasional triggering factors that facilitate landslides in the given area. The major triggering mechanisms that initiate landslides include seismicity, intense rainfall, and anthropogenic activities (Highland & Bobrowsky, 2008; Raghuvanshi et al., 2014).

2.2.2.1 Anthropogenic activities

In addition to natural-caused factors, anthropogenic actions are among the major triggering parameters that increase the likelihood of landslides. There is a high chance of landslides happening when human-driven activities such as road construction, mining, deforestation, urban expansion, cultivation, improper buildings, and agricultural reclamation are carried out (Li et al., 2020). In addition to these activities, excessive drainage of groundwater, excavation of construction materials, large-scale irrigation, and undercutting of the slope can aggravate the occurrence of severe landslides.

2.2.2.2 Intense rainfall

Prolonged rainfall is among the most important extrinsic elements for the happening of landslides through erosion, saturation, and an increase in soil weight. Most of the landslide hazards in Ethiopia were recorded during the wet season (Kifle Woldearegay, 2013). If an area experiences high rainfall, it has a high landslide susceptibility; while the rainfall amount decreases, the susceptibility also reduces (Li et al., 2020).

2.2.2.3 Seismicity

A landslide among the secondary natural disasters is associated with seismicity and ground shaking, potentially worsening the socio-economic impacts of the event (Valagussa et al., 2019). We can analyze the extent and distribution of landslides caused by an earthquake by considering various criteria such as lithology, local relief, proximity from the epicenter, and ground motion (Valagussa et al., 2019). As ground motion rises, the size and distribution of landslides increase, and as one moves farther away from the epicenter, there is less chance of greater landslides occurrence. Seismic activity may be accountable for new landslides or reactivating the existing ones (Kanungo et al., 2009).

2.3 Landslide susceptibility mapping approaches

As noted by Varnes (1984), a landslide hazard as the possibility of a devastating landslide occurrence occurring in a particular area at a certain time. Landslide hazards are the foremost frequent natural disasters, especially in hilly terrain, causing significant impacts on many resources, destruction of annual property, injuries, and fatalities (Kanungo et al., 2009; Kaur et al., 2017). Although it may not be possible to completely prevent the hazards posed by landslides, the

extent of damage can be reduced or compensated. The hazards emanating from landslides might not be entirely avoided, but the extent of damage can be minimized or compensated. Therefore, to minimize the damage to property and the loss of life, hazard zoning is one of the crucial techniques to create a safer environment (Das et al., 2022; Kanungo et al., 2009). Landslide susceptibility mapping denotes the method of partitioning the area into regions and assigning a grade to each area according to the level of current or potential landslide hazards from the area (Anbalagan, 1992; Varnes, 1984). Thus, it will aid planners in choosing suitable site selections for infrastructure, buildings, and lifeline facilities, as well as help to put prevention methods in the mitigation stage (Anbalagan, 1992). Various researchers used different approaches for landslide susceptibility mapping. However, the most well-known techniques used by many researchers are categorized widely into qualitative and quantitative (Das et al., 2022; Kanungo et al., 2009; Leulalem Shano et al., 2020; Tyagi et al., 2022). The researchers may select the appropriate approach based on the data available, the purpose of the investigation, the type of landslide, the researcher's skill, the accessibility, and the size of the research area (Leulalem Shano et al., 2020).

2.3.1 Qualitative approach

Qualitative techniques depend on the evaluator's knowledge, experience, and personal judgment of hazard investigation (Kaur et al., 2017). This approach uses data that is not numerical and a high amount of subjectivity nature is employed to generate many thematic data related to landslide incidents (Tyagi et al., 2022). Thus, the quality of a result is mainly determined by the expert's skill and interpretation ability. Geomorphic technique, inventory analysis, and expert evaluation are grouped under this approach (Das et al., 2022). The main weakness of these approaches is precise weightage of various conditioning factors may not be assigned. Because the rating is given based on the expert opinion in the field. Due to this the method reflects a high subjective nature and requires good skill and experience.

2.3.1.1 Geomorphic technique

The geomorphic approach examines the physical features of the earth to determine the areas that are vulnerable to landslides. This approach is a direct technique of landslide susceptibility mapping which requires good experience and interpreting capability of the investigator, to identify the existing and potential landslides in a particular area (Das et al., 2022). The information is gained via aerial photographs, field data, and geological maps (Leulalem Shano et al., 2020). Geomorphic

technique has certain limitations due to its heavy reliance on the evaluator's judgment and challenges in covering wide areas (Das et al., 2022). Only a field-based geomorphic approach can lead experts to misconceptions in areas such as dense vegetation, hills, and obscured old landslides (Kaur et al., 2017).

2.3.1.2 Expert evaluation techniques

These techniques require the professional knowledge, experience, and judgment of the evaluator to evaluate a potential landslide in a particular area. It includes a heuristic and inventory analysis approach (Fall et al., 2006). Inventory mapping is among the direct techniques for the identification and recording of landslides which is done by collecting past landslide incidents in a specific region (Leulalem Shano et al., 2020). The site, type, displacement, and extent of the existing landslide event can be recorded during inventory analysis. The GPS point data of the past landslide event is incorporated, to show the geographic distributions of landslide activities. This information can be documented via field surveys, historical records, aerial photographs, interviews, and satellite images (Tyagi et al., 2022). Nowadays thanks to technology and the advent of remote sensing and GIS helps us to take satellite images for better interpretation about the location, volume, extent of damage, and occurrences of landslide hazards (Das et al., 2022). Inventory mapping does not take into account the possible causative factor for landslide hazard assessment (Das et al., 2022). Expert opinions are employed in the heuristic technique to evaluate the potential landslide hazard in a specific area (Dai et al., 2002).

2.3.2 Quantitative approach

It comprises applying statistical or data-driven models to ascertain the likelihood of landslides in a specific area (Das et al., 2022). It consists of many methods viz; statistical, deterministic, probability, and machine learning approaches (Leulalem Shano et al., 2020).

2.3.2.1 Statistical approach

This approach involves the interactions between the likely causing elements and the landslide occurrences. It is constructed for regions where landslides are not yet occurring, but where comparable circumstances exist (Dai et al., 2002). This approach can be developed by determining the existing landslide events and each casual factor's relative contribution in a given area. Due to the utilization of such data, it reduces the subjective nature of the investigator, and the outcome is

mainly determined by the data's quality. Gathering more data within a large amount of area will be the main problem in statistical methods (Van Westen et al., 1997). It can be either bivariate or multivariate (Kaur et al., 2017).

A. Bivariate analysis

In this analysis, every causative factor is contrasted with an inventory map, and every component is ranked and determined according to their relative contribution based on landslide frequencies within the class factor (Kaur et al., 2017). The broad premise of this approach is that ″the past and the present are the keys to the future″ (Dai & Lee, 2001). This denotes that the same factors that were causing the landslides that are already occurring might very well cause landslides in a particular area. In bivariate analysis, each possible causative factor is determined and overlaid over the area's inventory map (Leulalem Shano et al., 2020). It includes the weight of evidence, certainty factor, frequency ratio, and information value (Kaur et al., 2017; Leulalem Shano et al., 2020).

B. Multivariate analysis

Multivariate statistical analysis takes into account the comparative contributions of every factor class to the overall susceptibility in a specific area (Kanungo et al., 2009). This method calculates landslide proportions in each pixel, generates landslide presence or absence, and classifies areas into different susceptibility classes (Leulalem Shano et al., 2020). Logistic regression, discriminant method, and machine learning approaches are among the most commonly employed techniques of multivariate statistical analysis (Das et al., 2022). The primary drawback of multivariate analysis is that the combination of different factor classes with an inventory map will lead to inaccurate interpretation, and the data inputs are more complex and consume a lot of time (Kanungo et al., 2009).

2.3.2.2 Deterministic approach

This method is also known as a physical-based model and it utilizes laboratory experiments to ascertain the slope's stability in a specific area (Kaur et al., 2017). A deterministic approach helps to evaluate the likelihood of a landslide in a certain area using a physical model (Fall et al., 2006). It solely involves slope stability, which indicates a safety factor, and it doesn't consider causative factors viz; vegetation, drainage, climate, and anthropogenic factors (Kaur et al., 2017). Due to the

accuracy and integrity of data at a large scale, the deterministic approach is commonly used in engineering design (Raghuvanshi et al., 2014).

2.4 Related previous works on landslide susceptibility mapping in Ethiopia

Owing to the progressively rising frequency of landslide hazards, several scholars have used various techniques to evaluate and map landslides. In this paper, some notable literary works that are closely associated with the purpose and methodology selected for this study are assessed. Several studies have used various methodologies to evaluate and map landslide susceptibilities in different areas of Ethiopia. The researchers including Dawit Asmare (2023); Leulalem Shano et al. (2021); Matebie Meten et al. (2015); Tadele Melese et al. (2022) used a frequency ratio method to evaluate and zone landslide hazards.

Leulalem Shano et al. (2021) conducted research to assess landslide susceptibility in South Ethiopia, particularly Gamo Highland. The researchers utilized a frequency ratio model to delineate the area to different susceptible classes. In this research, the authors considered nine conditioning elements including LULC, slope, elevation, aspect, lithology, curvature, proximity to stream, proximity to lineaments, and groundwater. The outcome of their work reveals that frequency ratio has a high predictive ability to categorize the area into different susceptibility classes.

Dawit Asmare (2023) also conducted research to assess landslide susceptibility around Choke Mountain, northwestern Ethiopia. To assess and map landslide in the region, the researcher used a frequency ratio and AHP methods. Lithology, elevation, aspect, slope, NDVI, distance to drainage, profile curvature, distance to road, and plane curvature were the causal elements that the author took into consideration. The results of the study demonstrate that the area is categorized as having very high, high, moderate, low, and very low susceptibility classes.

In the Debresina area, central Ethiopia Matebie Meten et al. (2015) conducted research employing frequency ratio and logistic regression approach. The researchers used slope, aspect, distance to fault, distance to river, lithology, curvature, elevation, and rainfall as conditioning factors. Other scholars including Azemeraw Wubalem (2020) and Filagot Mengistu et al. (2019) employed the information value approach to produce LHZ map. Their work demonstrates that the selected method accurately predicts the area into different susceptibility classes.

Therefore, in this research, bivariate statistical IV and FR models are preferable approaches to achieve the ultimate objective. These models utilized data about the existing landslides and predicted the area based on training landslides. The methods employed, conditioning factors, and scale of analysis in the above literatures are aligned with the general site conditions of the study area.

CHAPTER III

OVERVIEW OF THE STUDY AREA

3.1 Location and Accessibility

The study area is found in the eastern part of the Amhara regional state of the South Wollo administrative zone. It is located about 461 km from Addis Ababa and 61 km from Dessie, which is the capital of Ethiopia and South Wollo Zone respectively. Geographically, it is boarded between 558000–573200 m E and 1264300–1274400 m N and covers a total area of 100 km² (Fig. 3.1). For actual field investigations, it is accessible via the asphalt road. There are also many gravel roads to reach the desired traverses during the fieldwork.

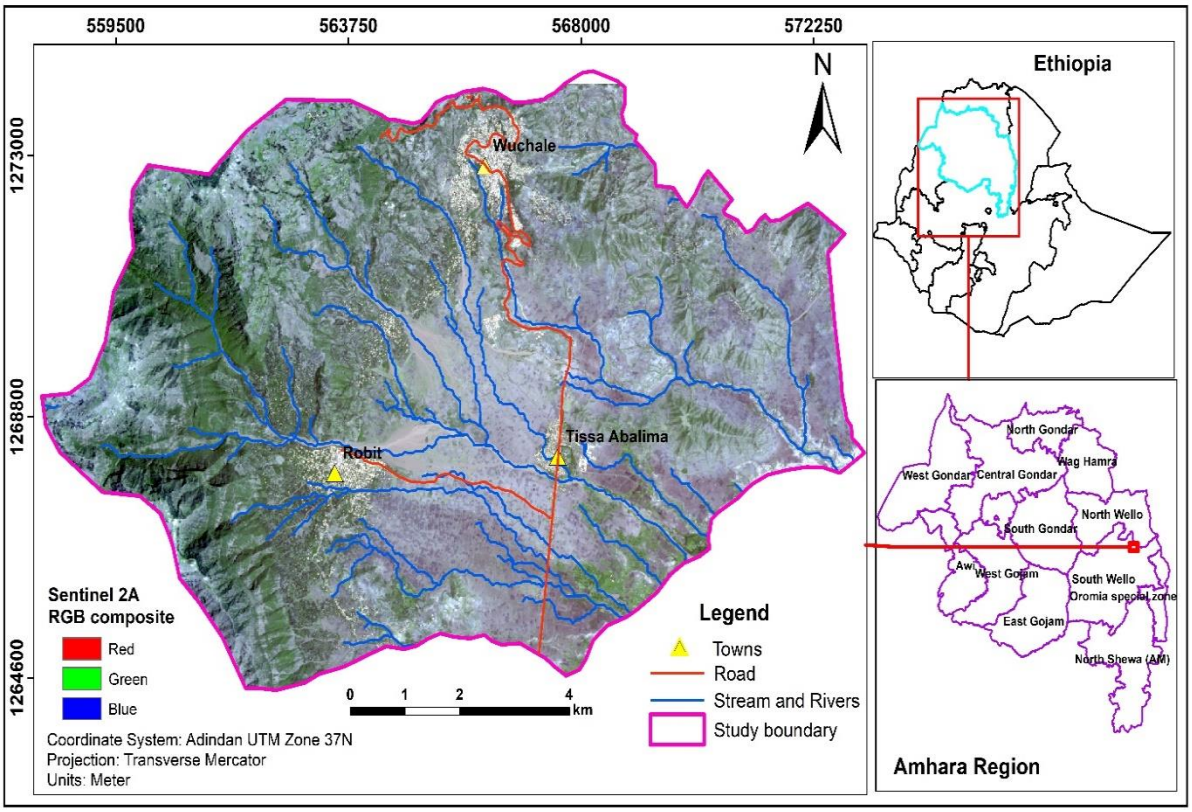

Figure 3.1: Location map of the study area.

3.2 Topography

The research area is distinguished by its intricate topography, varying from lowland plains to rugged terrain. The northwestern side of Wuchale town is dominated by a high elevated plateau

known as the Ambasel Ridge. In contrast, the southern segment of the region has almost flat terrain. The area encompasses steep mountain ridges, gorges, valleys, and grabens. Elevations in the investigated area range from 1400 to 3500 meters (Fig. 3.2). The elevation difference within the area is considerable and measures 2100 meters. These varying elevations contribute to the diverse landscape of Wuchale, impacting factors such as agriculture, transportation, and settlement patterns. The geomorphology of the area is heavily influenced by both alluvial and colluvial processes, with soil and rock materials gradually moving towards the flatter regions as indicated by the blue area in Fig. 3.2. Consequently, areas at higher elevations are significantly prone to landslides and stream erosions, especially in the rainy season. Most active landslides and landslide scars are prominently observed in the steeper part of the research area.

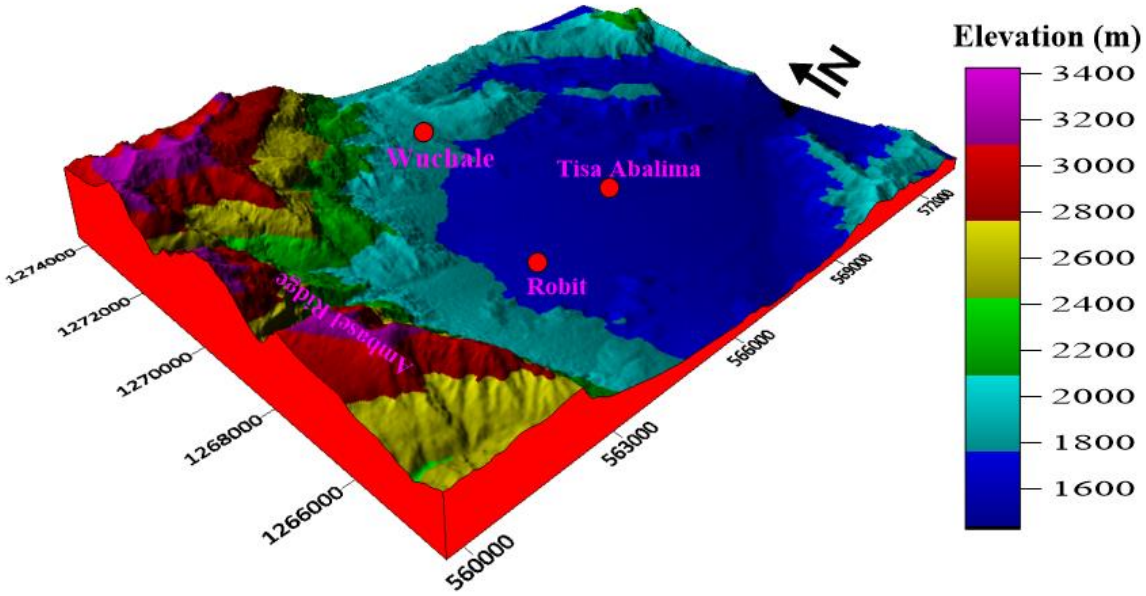

Figure 3.2: Physiography map of Wuchale area

3.3 Drainage

The area is a portion of the lower Awash Basin, with streams and rivers flowing into the upper Mile River catchment. Dendritic streams flow from the Ambasel ridge towards the Ajewa River, passing through Robit town before ultimately joining the Mile River. Aromba and Ajewa Rivers are the main rivers in the area, with all streams feeding into them. The drainage system of the area is described by its dendritic nature, where tributaries flow from high elevations such as the

Ambasel ridge towards the plains (Fig. 3.3). Most streams originate from the northwestern side of Wuchale town. Intermittent rivers are common, with water present during the summer season but drying up in winter, except for the Ajewa River. Landslides and erosional surfaces are frequently observed along the paths of these streams.

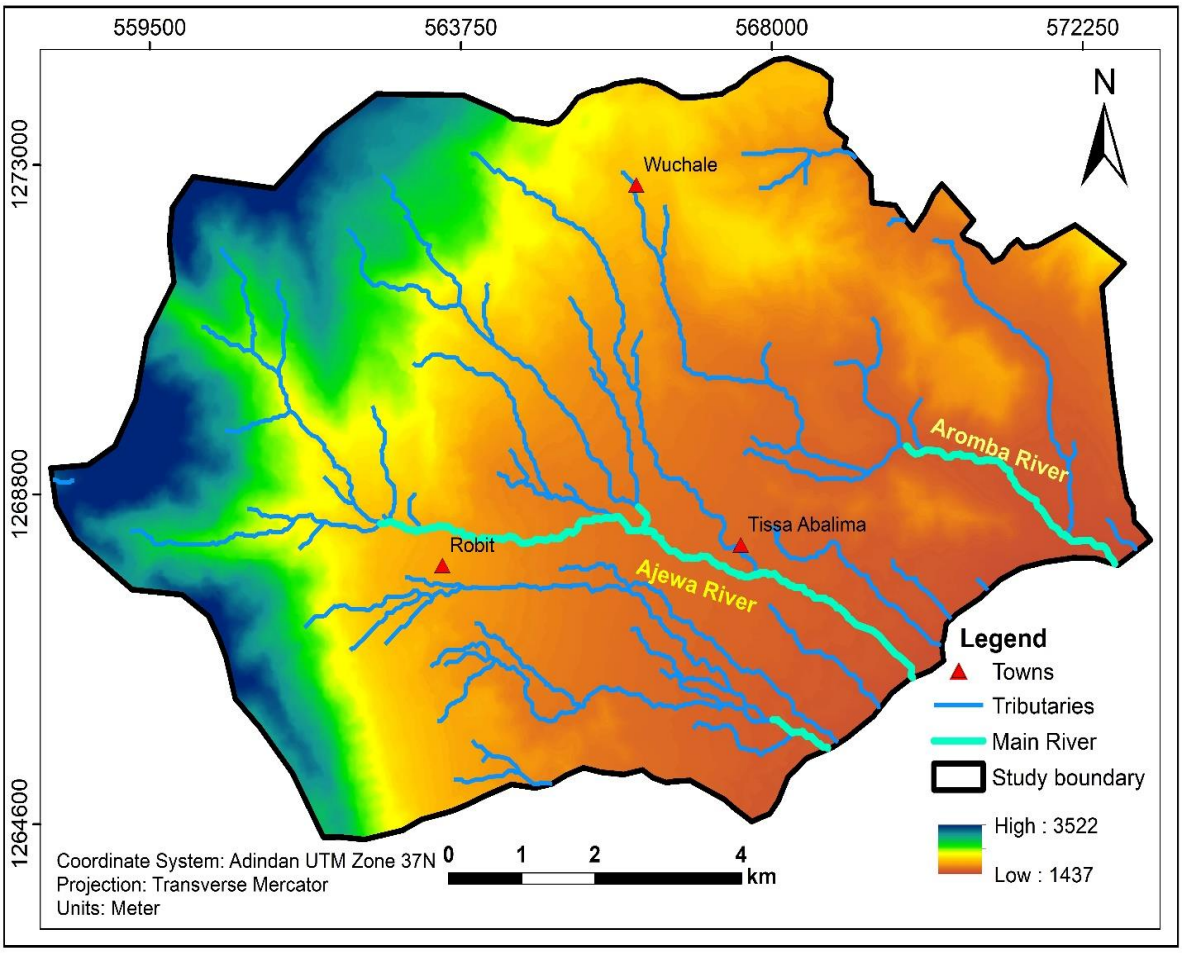

Figure 3.3: Drainage map of Wuchale area.

3.4 Climate

Climate can have a great influence in triggering landslide in a particular area. Ethiopia experiences diverse climatic conditions across its different regions. Highland areas typically receive rainfall perennially, whereas lowland areas tend to be dry. A prolonged rainfall and temperature variation can influence the stability of slopes in these zones. In the area known as Qina Amba, debris slides are common after a prolonged rainfall in the area. The rainfall saturates the soil and reducing the soil cohesion, triggers slope failure. The area obtained an annual average rainfall of 1146.825 mm

from the year 2000–2015. In Wuchale station the highest amount of precipitation was recorded in 2010 with a value of 1643.6 mm. The average rainfall in Mersa station is recorded at 897.04 mm. In Mersa station the highest precipitation was recorded in the year 2018 (1352.8). The minimum and maximum value of average monthly precipitation is observed in February and August for both stations (Fig. 3.4 b) respectively. The lowest and highest temperature is found in December and June correspondingly from the year 2000 to 2023 (Fig. 3.4 a). The precipitation and temperature data of the study area were gathered from the Meteorological Institute of Ethiopia. The meteorological data were collected from two stations (Mersa and Wuchale).

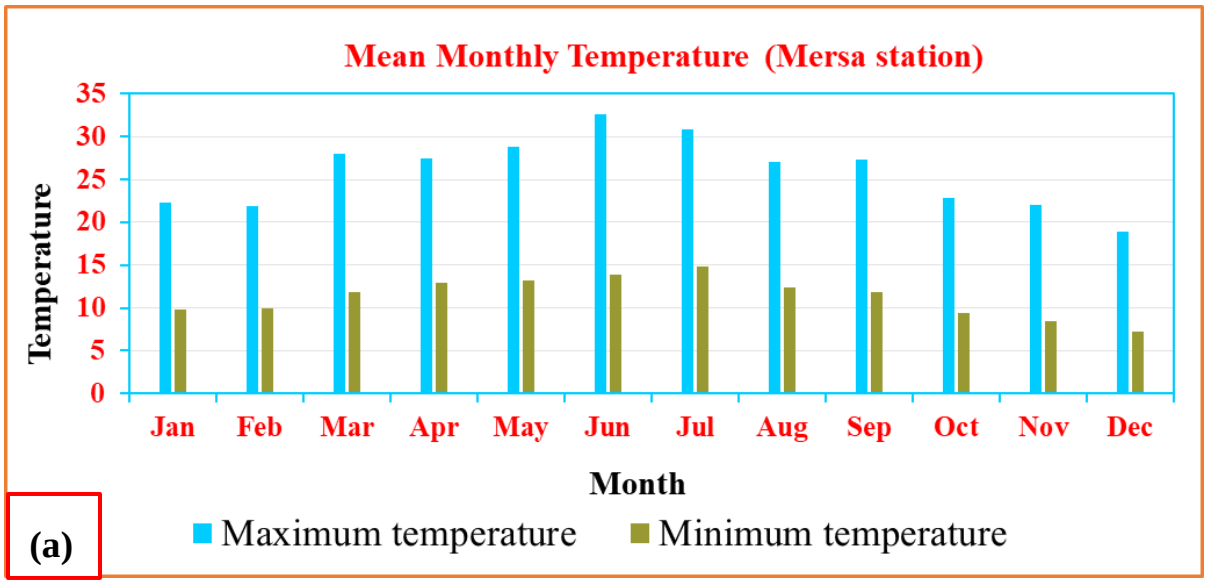

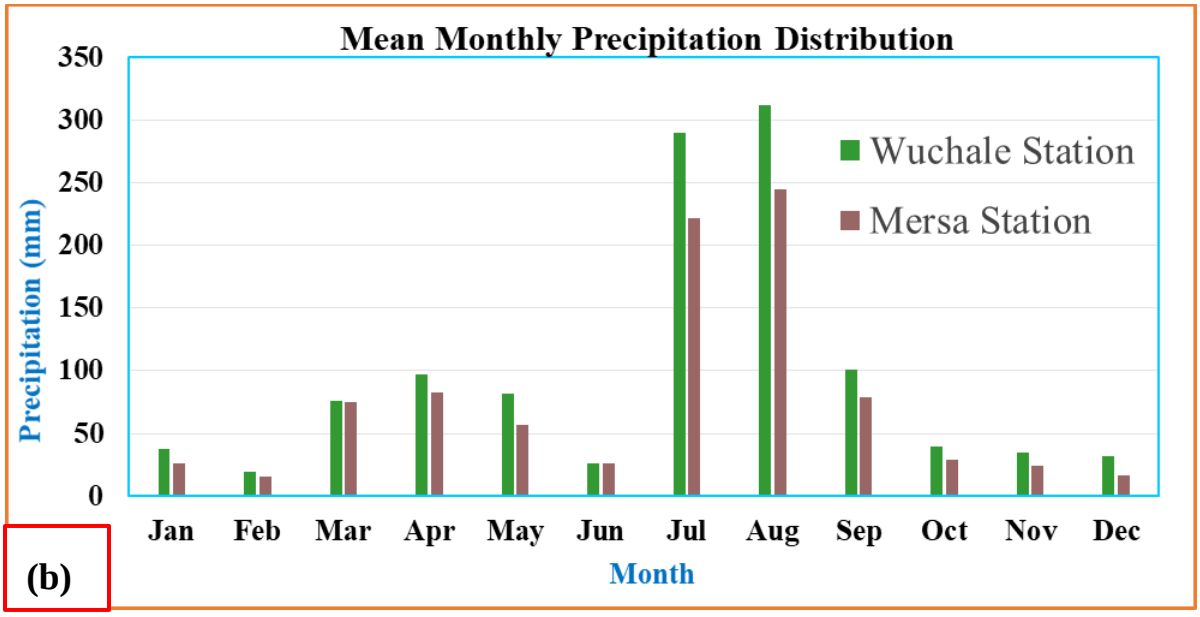

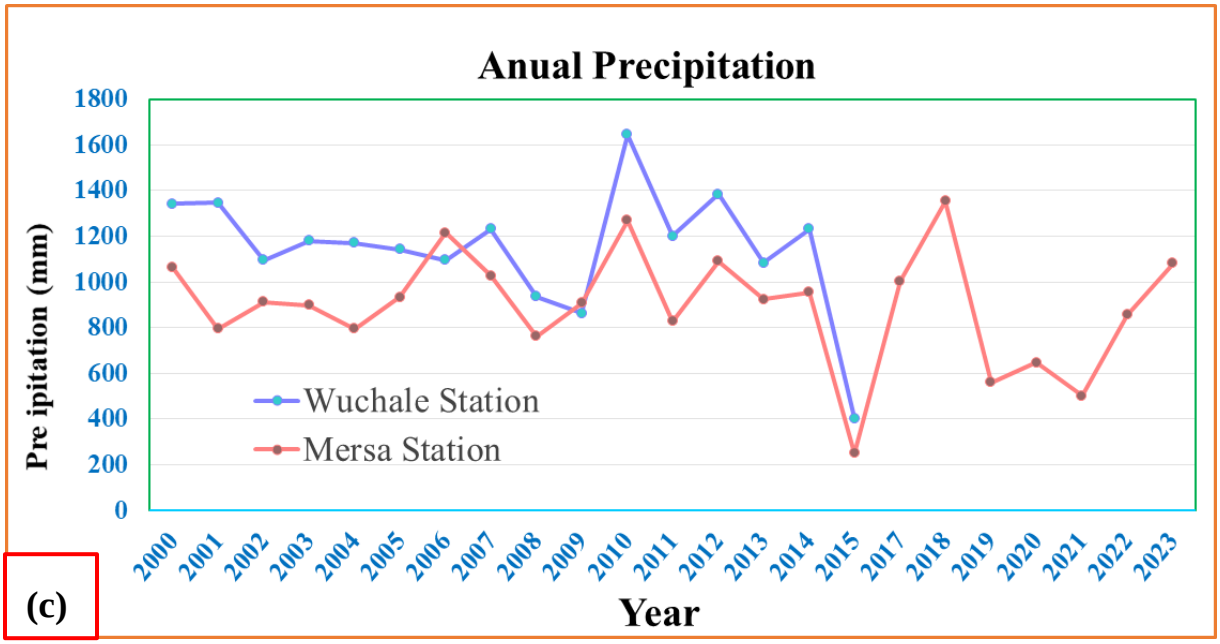

Figure 3.4: Precipitation and temperature graph.

Mean monthly temperature of Mersa station (a), Mean monthly precipitation distribution of Mersa (2000-2023) and Wuchale stations (2000-2015) (b), and Annual precipitation of Mersa and Wuchale stations (c).

3.5 Geology of the area

3.5.1 Regional Geology

Ethiopia's flood volcanic province erupted before 30 Ma, within a timeframe of less than 1 million years, covering an estimated area of approximately 600,000 square kilometers. This region is predominantly composed of mafic and acidic volcanic rocks (Hofmann et al., 1997; Mohr & Zanettin, 1988). The thickness of these volcanic layers fluctuates across different areas, with estimates reaching up to 2000 meters in certain regions (Mohr & Zanettin, 1988). Approximately 30 million years ago, the Afar mantle plume, spanning over 300,000 cubic kilometers, contributed significantly to shaping this CFB (Dereje Ayalew et al., 2002). The activity of this mantle plume has had profound effects on the development of various geological features in the region, including the Red Sea, East African Rift Valley (EARV), the Gulf of Aden, and the adjacent Afar depression. This activity has led to magma extrusion, uplift, and fragmentation of continental crust, thus shaping Ethiopia's landscape since the Oligocene period (Abbate et al., 2015).

The Ethiopian area had experienced extensive eruptions of trap successions following the deposition and buildup of Jurassic sediments, mostly in the Oligocene (Abbate et al., 2015). Several authors including Ebinger & Sleep (1998); Mohr & Zanettin (1988) noted that the trap successions expanded from the early Eocene to the Oligocene throughout the highlands in northwest and southern Ethiopia,

Ethiopia's volcanic regions were divided into five main categories by Abbate & Sagri (1980): northern, southern, Somali, Afar, and MER volcanites. The geology of the Wuchale area falls within the northern Ethiopian highlands. Therefore, this chapter will primarily focus on explaining the regional geological setup of flood volcanics of the northern Ethiopian plateau.

Various previous studies have indicated that the northwestern highlands are characterized by Oligocene to Miocene bimodal basaltic-rhyolite rocks. Investigations conducted by Beccaluva et al. (2009); Kieffer et al. (2004); Pik et al. (1999) in northern Ethiopia have identified Oligocene basalts as predominant. Further Dereje Ayalew (2011) has documented the presence of Miocene bimodal basaltic-rhyolitic rocks, succeeding the Oligocene Ethiopian continental flood basalt provinces.

Zanettin et al. (1980), classified the volcanic phases of the northwestern Ethiopian plateau into three periods, each phase consisting of one or more volcanic formations. These phases are delineated as before the Oligocene, between the Oligocene and Miocene, and from the Miocene to the Pliocene. Drawing from the eruption history (age), many researchers have grouped the area within Cenozoic volcanic succession, encompassing several major stages: 1). Pre-Oligocene, 2). Oligocene, 3). Oligocene-Miocene, 4). Miocene and 5). Quaternary volcanism/sediments (Fig. 3.5). This classification is dependent on the age data compiled from various sources and aligned with the geologic time scale.

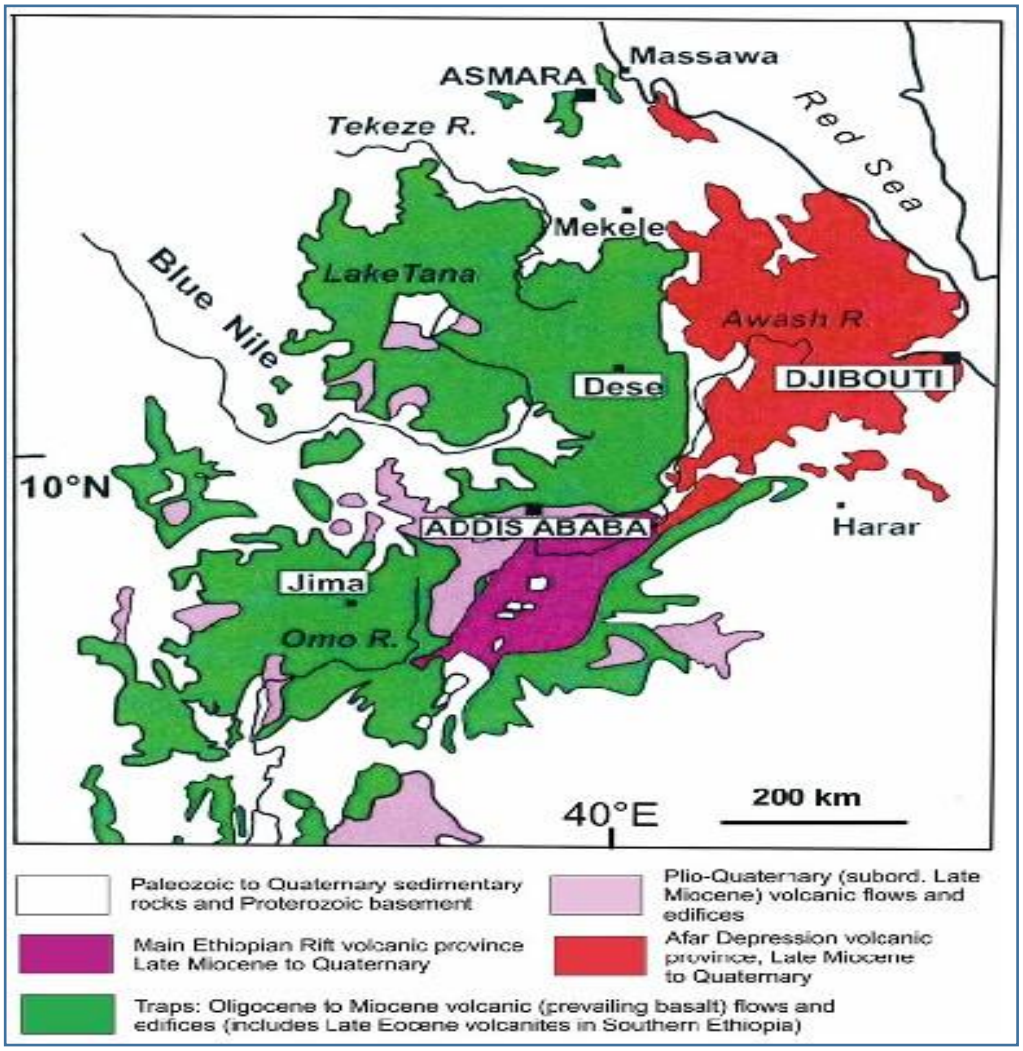

Figure 3.5: The main volcanic provinces of Ethiopia (Abbate et al., 2015).

Table 3.1: Generalized description of regional geology.

S.N	Formation	Description	Age
1	**Ashangi basalt**	The earliest fissure-fed Cenozoic plateau basalt volcanism in the region, is characterized primarily by basalts and occasional rhyolites (Mengesha Tefera et al., 1996). They occur unconformably beneath the Oligocene Aiba basalts and are signified by tilted, faulted, and highly weathered basalts (Zanettin et al., 1980). In the Dessie map sheet, these basalts reach thicknesses of approximately 1000 meters along the Beshilo river section, gradually decreasing to less than 200 meters towards the Dessie-Kombolcha road. The oldest estimated age is approximately 54 million years (Kazmin, 1979).	Pre- Oligocene
2	**Aiba basalts**	Exhibit a common aphyric texture, occasionally displaying porphyritic characteristics (Gezahegn Yirgu, 1997). These basalts overlay the Ashangi basalts unconformably, reaching thicknesses of approximately 0.2 to 0.6 kilometers. They were formed during the Oligocene period, with ages ranging from 34 to 28 million years (Mengesha Tefera et al., 1996; Zanettin et al., 1980)	Oligocene
3	**WogeleTena Rhyolitic-Ignimbrite**	It is mainly composed of acidic varieties of Oligocene formation that occurred overlain on the flood volcanic succession (Dereje Ayalew et al., 2002; Hofmann et al., 1997). Defines distinctive plateau topography, reaching a maximum thickness of 0.5 kilometers, significantly eroded and dissected by steep rivers (Dereje Ayalew et al., 2002; Tesfaye Demissie et al., 2010). It is mainly outcroped in Wogel Tena town, along the Dessie-Tenta Adjibar road, and in the Gishen and Ambassel ridges. Erupted approximately 30.2 Ma (Hofmann et al., 1997).	Oligocene

4	**Tarmaber Guassa formation**	Which erupted between 26 and 16 Ma, representing an Oligocene-Miocene basaltic shield volcano (Kazmin, 1979). Predominantly comprises alkaline to transitional basalt. Considering their eruption ages, the Semien Shield Volcano (18.85 Ma), Guguftu Shield Volcano (22.3 mega annum), and Choke Shield Volcano (22.4 Ma) fall into this formation. The eruption timeline of the Tarmaber Guassa formation has been documented by (Kieffer et al., 2004).	Oligocene - Miocene
5	**Alaji formation**	Found predominantly in the form of ignimbritic sheets. The rocks from the Alaji formation are acidic in composition and exhibit restricted variations. It exhibits an age range from 31-13 Ma (Zanettin et al., 1980)	Oligocene - Miocene
	Dessie Basalt Formation	Overlying on the Ashangi basalt and well exposed in the Tossa mountain chain, areas that follow the escarpment of the Jita and Gerado rivers (Tesfaye Demissie et al., 2010). Ukstins et al. (2002) determined the age of basalt from the Dessie-Bati section is estimated to be ~25 Ma, dated using $^{40}Ar/^{39}Ar$.	Oligocene - Miocene
6	**Tarmaber Megezez Formation**	The name was given to the younger shield volcano that erupted from 16-13 Ma during the Miocene stage (Kazmin, 1979). They predominantly consist of basalts and intermediate varieties (Gezahegn Yirgu, 1997). The Megezez formation is comprised of shield volcanic basalts dominated by porphyritic textures with transitional compositions (Birhane Girum et al., 2023).	Miocene

3.5.2 Local geology

This study lies within the northwestern Ethiopian plateau, specifically within the rugged topography of the Ambasel ridge. Here, diverse lithological units are exposed, encompassing rhyolitic, ignimbrite, and basaltic formations on the top and unwelded tuff, alluvial deposits, and colluvial deposits on the bottom section (Fig. 3.10 a). These lithological units are well exposed along the road cuts, hillside, and flat land exposures. Geomorphologically, the area is eroded by streams and rivers originating from the Ambasel ridge, resulting in a dissected terrain marked by erosional features. The intermittent River is widely seen in most of the study area. Along these river courses alluvial deposits are observed on the flat laying terrain.

3.5.2.1 Ignimbrite

Ignimbrite is among the lithological units exposed in the research area. It is particularly exposed in the northern and northwestern parts of Wuchale town. This type of lithological unit is well exposed by a road cut exposure towards the Ambasel section. Its color ranges from gray to light gray. It is identified by the presence of clasts and lithic fragments, which are easily identified by the naked eye within hand specimens (Fig. 3.6 b). The degree of weathering exhibited by this rock spans from moderate to high. Notably, in areas such as Graar Genda in Wuchale town, ignimbrite is covered with colluvial deposits and exposed after an extensive landslide happened in the area.

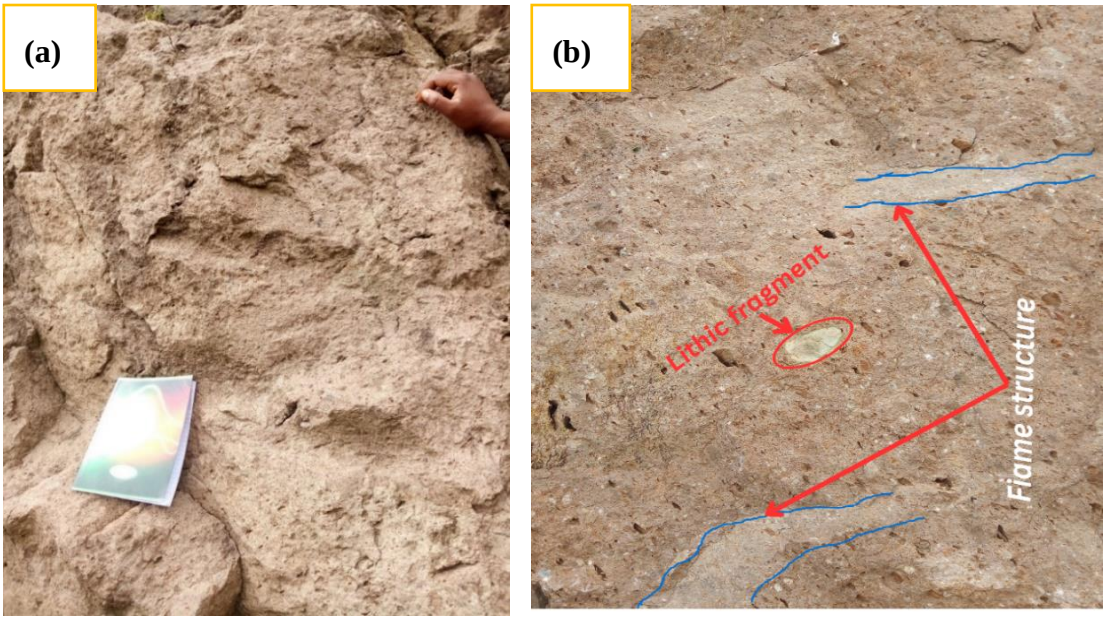

Figure 3.6: Unwelded tuff (a) and ignimbrite (b).

3.5.2.2 Basalt

The basaltic rock is highly exposed in the northern, western, and eastern segments of the research area. This unit is dominantly comprised of basalts of aphanitic and porphyritic textures with minor interlayered felsic-pyroclastic deposits towards the top succession. It is found overlaid by rhyolite on the Ambasel ridge near Wuchale town. It has light black–dark gray weathered and fresh color respectively. It is also characterized by a highly fractured, jointed, and intensely weathering nature (Fig. 3.7). The highly weathered rocks are altered and reflect a somewhat greenish color. The bulk of the research area is covered with basaltic units of varying composition and strength. In the northern and northwestern segments of the research area, the basalts are characterized as highly weathered, fractured, and jointed (Fig. 3.7 c). During field observations, most of the landslides in the area were documented from basaltic rock units in a sloppy terrain.

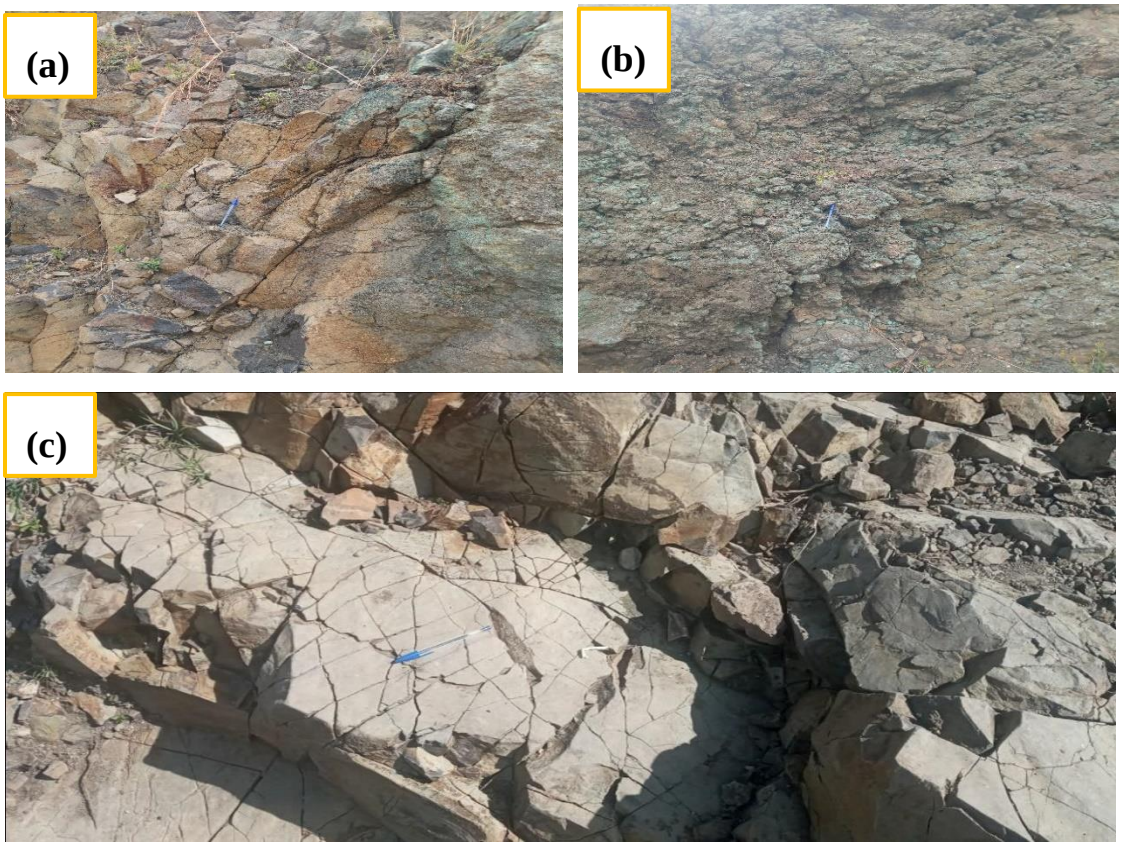

Figure 3.7: Basalts

Fractured and jointed basalt (a), highly weathered basalt with alteration (b), and basalts with different joint sets (c).

3.5.2.3 Rhyolite

Rhyolite is found on the top part of the investigation area, commonly known as the Ambasel ridge. It forms a continuous chain of ridges in the area near Robit town. It is found on the top of basalt formations. It has an approximate thickness of 100 m. It has yellowish and light gray weathered and fresh color respectively (Fig. 3.8). The observable banding flow nature is the main distinguishing feature to identify this lithology.

Figure 3.8: Rhyolite rock which shows banding flow.

3.5.2.4 Alluvial deposit

Alluvial deposits are highly exposed along the river pathway (Ajewa and Aromba) and floodplain. It covers the flat land area and is used as agricultural land for the local community, especially for irrigation purposes. The materials deposited comprised silt, clay, sand, gravel, and boulder-size particles (Fig. 3.9 a). These particles are transported from their location by the action of water, especially throughout the rainy period, and are later deposited on the flat land terrain. Even though they are loose and unconsolidated materials, there is not significant landslide observed in alluvial deposits found in the flat terrain. Areas found in the vicinity of the streams are covered with alluvial sediments and hence they are more prone to landslide.

3.5.2.5 Colluvial deposit

Colluvial soils are deposited on the bottom lowland area and make up the majority of the study region. It consists of fine-grained silty, clay and sand with a minor amount of gravel materials. The materials are deposited due to the action of weathering and transported from the sloppy terrain towards the plain (Fig. 3.9 b).

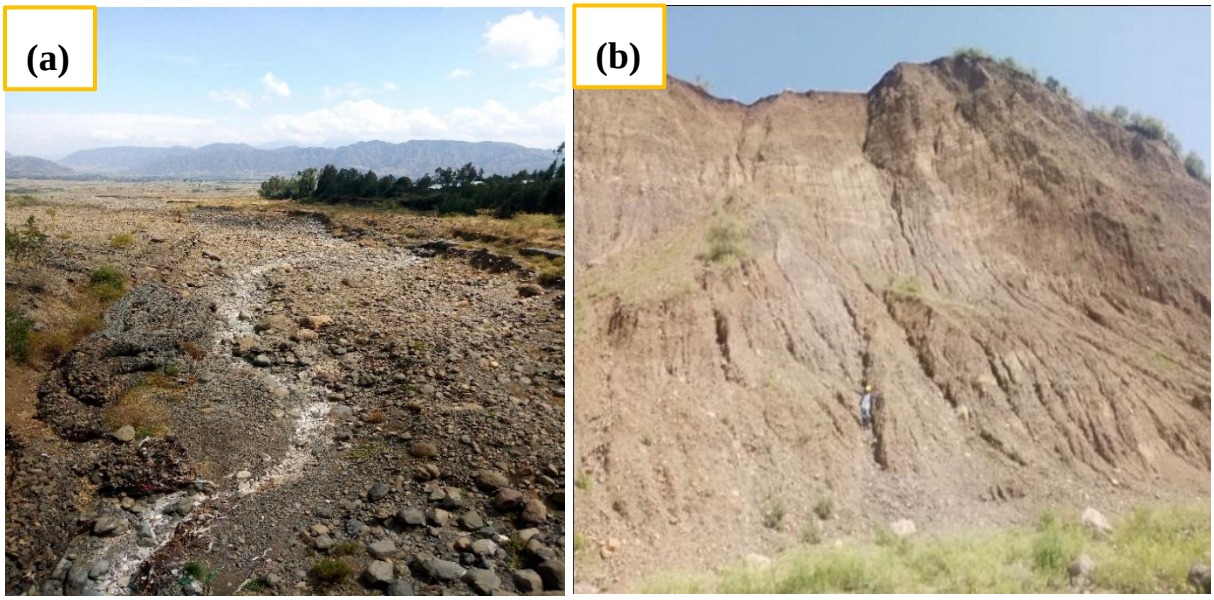

Figure 3.9: Alluvial soils (a) and colluvial soils (b).

Table 3.2: lithology class.

		Area covered	
S/N	Lithology	Area (Km^2)	Area (%)
1	Aiba Basalt	21	21
2	Rhyolite	11	11
3	Alluvial and Colluvial deposit	43	43
4	Ignimbrite	2	2
5	Ashangi basalt	23	23
Total		100	100

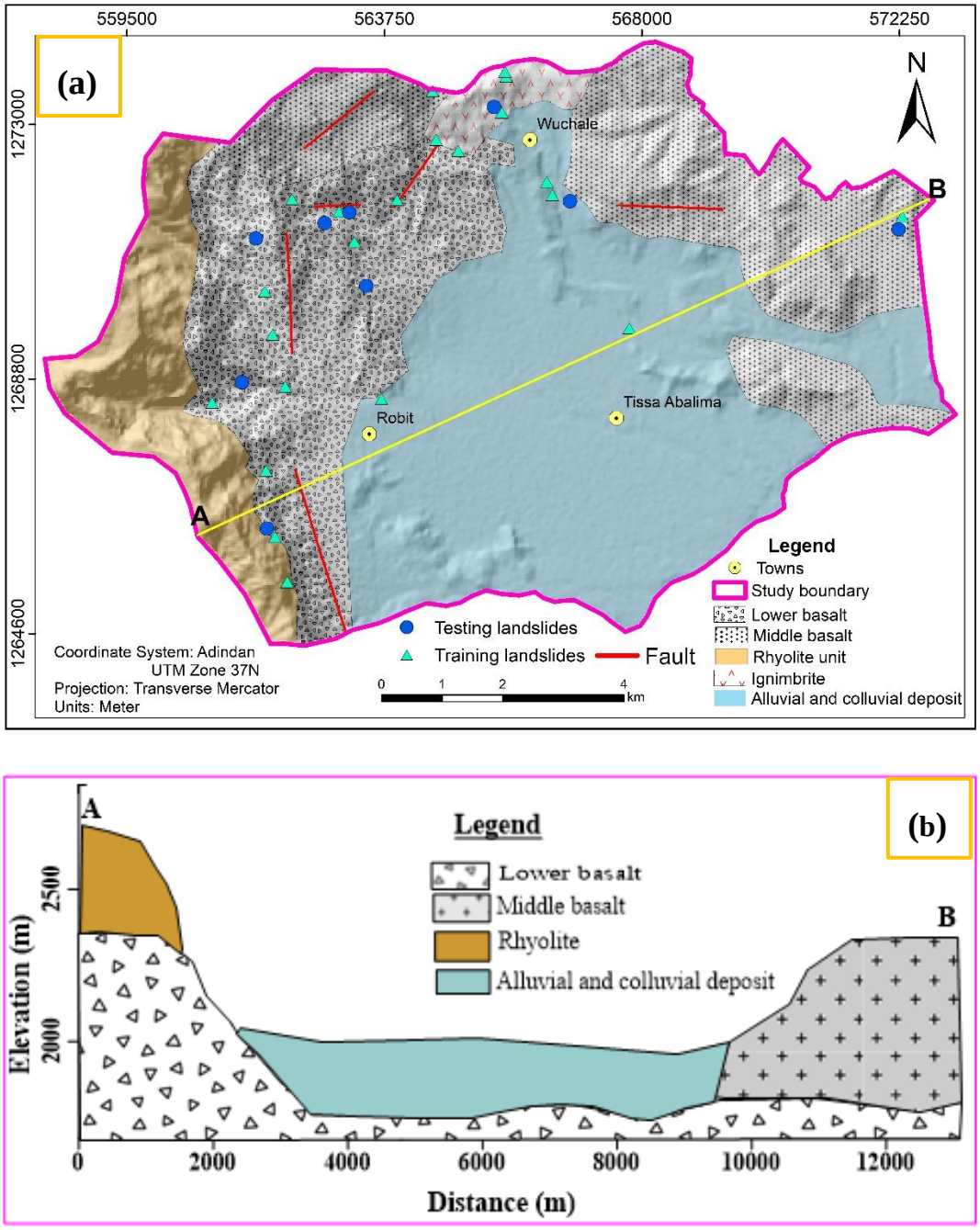

Figure 3.10: Geological map of the Wuchale area (a) and geological cross-section (b).

3.6 Hydrogeology

Hydrogeology controls the frequency of landslides in a specific area. Water can easily circulate through weak zones and pore spaces. In the study area, many springs and streams can facilitate the frequency of landslides. Most of the springs in the study area are found at the bottom of hills,

ridges, already sliding areas, and along fault escarpments. Some of the springs were formed after the landslide activities had occurred (Fig. 3.11 a). According to the local community, there was a landslide 20 years ago, and after the landslide occurred, springs formed. This indicates that hydrogeology is one of the controlling factors for the formation of landslides.

Figure 3.11: Springs

Formed after a landslide occurred in Graar genda (a) and spring on the bottom of landslide area near Wuchale town (b).

3.7 Failure mechanism in the study area

Several variables, including geology, geomorphology, and human activity, can cause landslides (Varnes, 1978). Different systems of classification for landslides are in place, depending on the kind of material and how it moves. As a result, Varnes (1978) classified landslides as complex movements, falls, topples, slides, spreads, or flows. The study area's most frequently observed failure mechanisms include falling, rotational slide, and debris slide.

3.7.1 Debris slide

These are mainly observed on the rugged terrain of the Wuchale area, particularly around Qina Amba and Robit (Fig. 3.12). They are mainly moved in the rainy season and cause more damage in the farmlands. It was prone to slides during the rainy period and comprised of fine-grained sediments to coarse gravel rocks. The area was cropland before it began sliding. The majority of

the steep slope part of the study area is covered with debris slide. Both the natural and human interventions were the main triggering factor. The slope materials are highly disturbed due to agricultural activities in the area. Subsequently, by the effect of rainfall and stream action the area were undergo sliding. Fig. 3.12 illustrates debris slide in the research area, the images were taken from Google Earth Imagery captured on November 2, 2022.

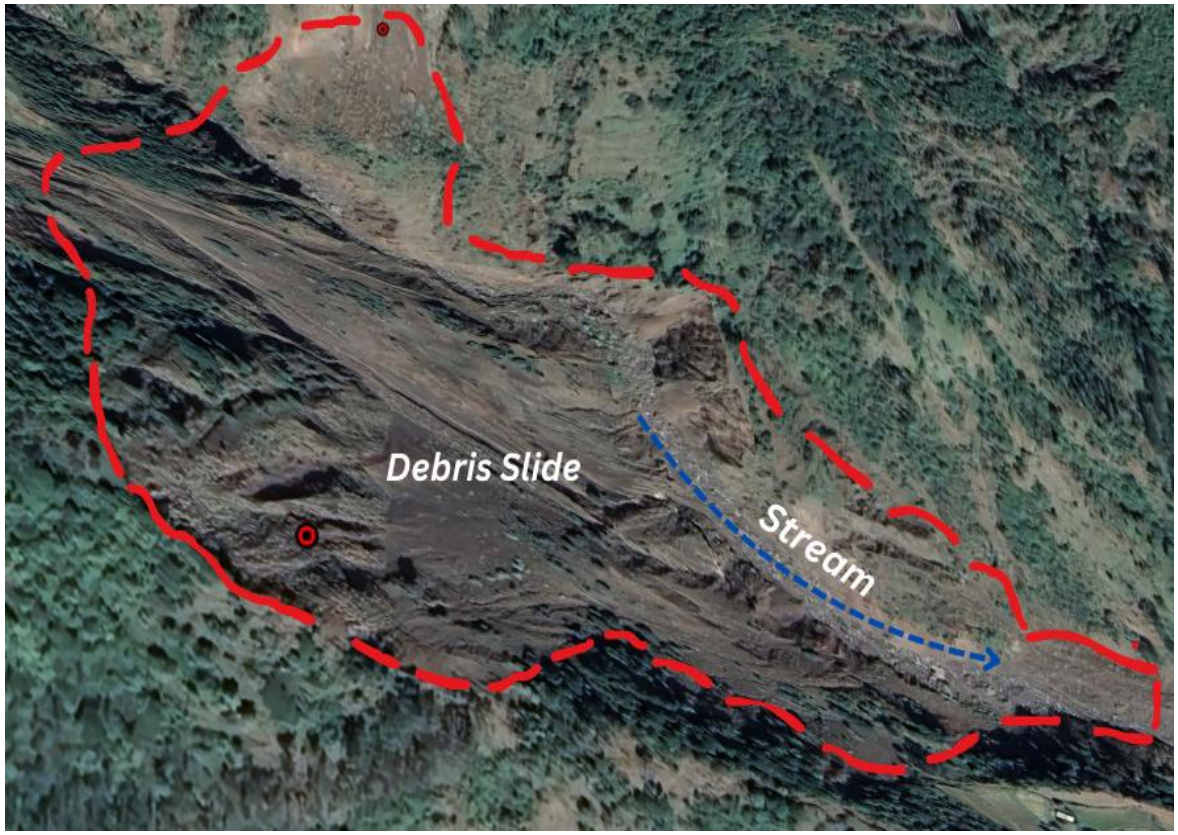

Figure 3.12: Debris slide in Qina Amba.

3.7.2 Rotational slides

Such type of slides are commonly happened in flat terrain such as those observed in the Wuchale town, particularly in the Graar Genda area. In the research area, rotational slides exhibits a vertical displacement in which the materials moves along a concave-downward slip surface (Fig. 3.13). The common sliding materials observed are black cotton clay and pyroclastic deposits. The clay materials are found on the surface of the earth, while the pyroclastic deposits are exposed after the surface were sliding. The vertical displacement is measured about 20 m. All the buildings, vegetation, and electric poles were moved along with the surface.

Figure 3.13: Rotational slide in Graar Genda.

3.7.3 Rock falls

These types of movements are found in the Dembot area. The boulder-sized rock was detached from the host rock after the slope was excavated for road construction. These events were triggered by human interventions, and have become notably prevalent following extensive excavations for road construction. The geological materials of the area are dominated by a combination of unwelded to welded tuff and highly weathered basalt. The block of rock is detached from the parent rock and moved without continuous contact with the failure plane (Fig. 3.14 a).

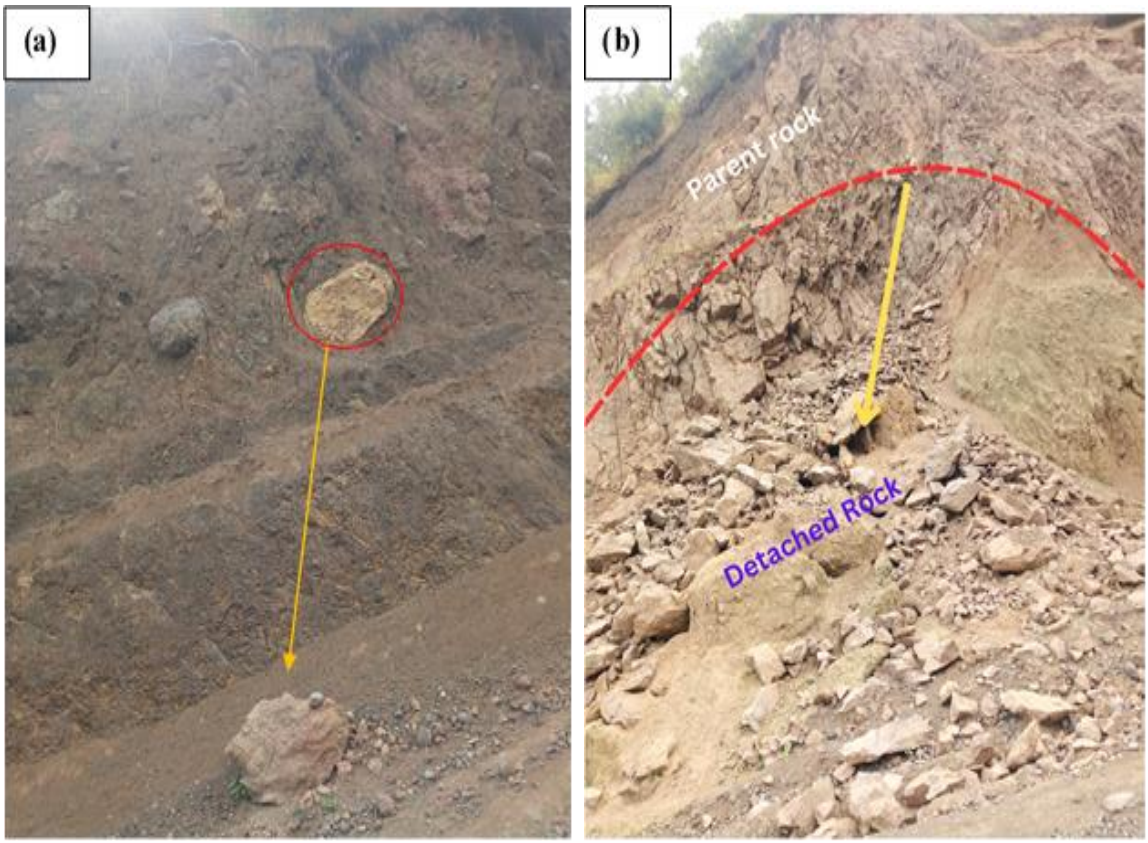

Figure 3.14: Rock fall in Dembot area.

3.8 Extent of damage in the study area

In December 2022, a catastrophic landslide occurred here, causing significant damage. A shocking 174 homes were completely demolished, forcing 533 families to be evacuated from their homes. Even now, houses near the landslide site still show cracks during on-site surveys, indicating the ongoing danger posed by such events. The landslide covers around 9 ha. All the houses, electric poles, water pipes, and vegetation are damaged. Even the deep rooted Eucalyptus also moved along with the surface. A huge surface crack measured about 2 m deep and widen by 2.5 m was observed in the area. In addition to the destruction of houses, life line infrastructures (electric poles, cables, and water pipes), vegetation, and roads were demolished in the area (Fig. 3.16).




Figure 3.15: Demolished houses in Graar Genda

Figure 3.16: Damaged infrastructures.

Failed electric pole after a severe landslide happened in Graar Genda (a), damaged electric cable at Graar Genda (b), and Damaged asphalt road at Aromba area (c).

CHAPTER IV

METHODS AND MATERIALS

4.1 Introduction

Several techniques have been applied to landslide susceptibility mapping by different researchers. The methods proposed for landslide investigation are categorized broadly into qualitative and quantitative approaches (Das et al., 2022; Kanungo et al., 2009; Kaur, 2017; Leulalem Shano et al., 2020; Tyagi et al., 2022). The researchers say qualitative approaches are conducted through knowledge-based experience and field observations. Conversely, quantitative approaches are data-driven, and the outcome relies on the data's quality. The literature review explains each of these methods well (Chapter II). This study applied a statistical bivariate information value and frequency ratio approach to prepare the final landslide susceptibility map. The methods are chosen depending on the area's extent, the aim of the investigation, and data availability.

4.2 Methodology

As stated by Van Western (1993), the scale of examination is critical in selecting the method for landslide investigation. This study covers 100 square kilometers and was conducted at medium scale of 1:50,000 (Fig. 3.1). This study applied a GIS-based bivariate FR and IV models to assess and classify landslide susceptibilities in the Wuchale area. Many researchers have stated that statistical methods are preferable for landslide susceptibility due to the low degree of subjectivity. Therefore, the results derived from these methods are mainly determined by data integrity. The methods were chosen reasonably based on the data available, the purpose of investigation, landslide type, the area’s size, and the model’s data-driven nature. GPS point data about the existing landslides were collected through field surveys and interpretations of Google Earth Images. The collected point data were then converted into polygons using Google Earth Pro and saved as KML files. Later, the KML file was transformed into layer and rasterized in the ArcGIS environment. Maps were created for each factor and overlaid on the landslide map. The pixels within each factor class were then counted based on the density ratio.

Slope, aspect, elevation, LULC, distance to stream, and lithology were the six parameters selected for the present study. Each causal factor was assigned to new classes and analyzed individually, and later combined to delineate the susceptible area. Each factor's relative contribution to

landslides was taken into account when assigning a rating. To conduct the study, three phases of procedures were followed including desk study, field investigation, and data processing stages.

4.2.1 Desk Study

This phase serves as the foundation for research efforts as it initiates the obtaining of essential materials, equipment, methods, and data collection processes. Key activities undertaken include collecting historical data and required field equipment from various sources. Base maps, consisting of topographic and geological maps, are obtained from reputable sources such as SSGI and GSE. Essentially, this phase involves the acquisition of various thematic maps, datasets, and equipment from various organizations and sources.

4.2.2 Field investigation

Field investigation serves as the primary procedure for studying the characteristics of landslide events including their failure mechanisms, types, extents, and precise locations. The characteristics of landslides were documented through careful observations and measurements in the field notebook. Key activities undertaken in this phase include selecting traverses across major lithological units to delineate rock unit boundaries, examining lithological unit properties via hand specimens and subsequently drafting local geological maps, collecting GPS points to existing landslides through both observation and interviews with the local community, and examining potential failure mechanisms of existing landslides were achieved.

4.2.3 Post fieldwork

These post-field investigation activities are crucial for synthesizing the gathered data effectively. This process encompasses several key steps: arranging the collected data into a usable format, transforming point data concerning past landslides into polygons and subsequently converting these polygon data into raster format, ensuring consistency in cell size values across inventory and factor maps, resampling and reclassifying each factor map before overlaying them onto the inventory map to count landslide pixels among every factor class. Values of FR and IV model of each factor was computed in an Excel sheet as per Eq. 1&3 respectively. Subsequently, the calculated IV and FR values were assigned to every factor classes by using look up tool in GIS. Using the raster calculator, each conditioning elements with corresponding values of FR and IV

were summed as per Eq. 2 and 7. After performing such activities the final susceptibility map was produced by verifying all factor maps within a GIS environment (Fig. 6.3).

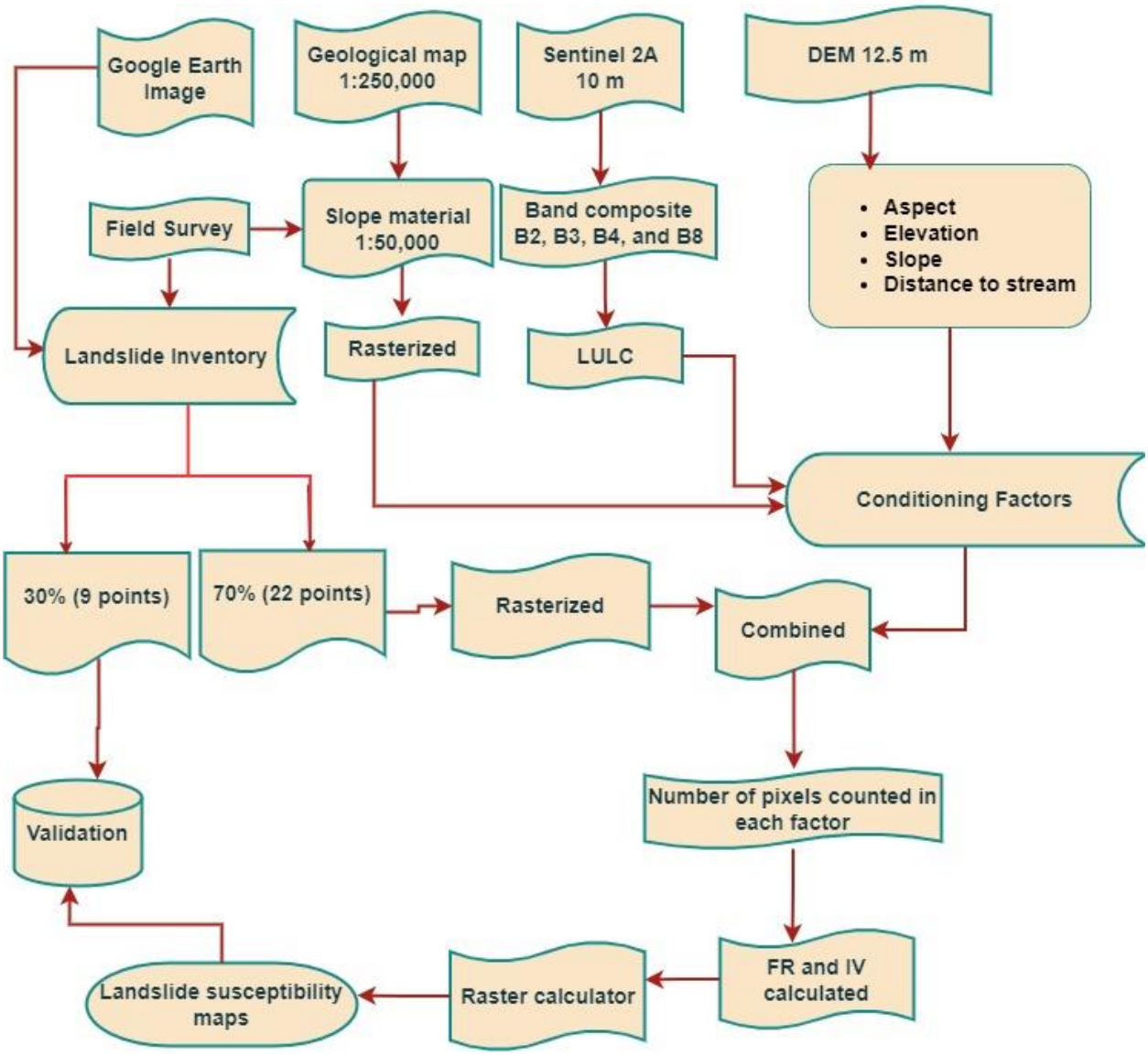

Figure 4.1: Methodology flow diagram.

4.3 Materials

To conduct the research different materials were utilized including handheld GPS, topographic map, field notebook, geological hammer, and compass. Additionally, ArcGIS 10.4, Google Earth Pro, Global Mapper, EARDAS IMAGINE 2014, Microsoft Excel, and surfer19 were utilized as a tool to collect, handle, prepare, and analyze the data.

Table 4.1: Datasets and their sources utilized in this research.

Data	Source	Data layer	Data format	Scale or resolution
Geological map	GSE, Dessie map sheet	Lithology	Vector/polygon	1:50,000
Topographic map	SSGI	Base map	Raster	1:50,000
ALOS PLASAR (DEM 12.5 m)	Downloaded from Alaska satellite facility https://asf.alaska.edu/	–Elevation –Slope –Aspect –Stream	Raster	12.5 m
Sentinel 2A images (10 m)	Downloaded from Copernicus website https://dataspace.copernicus.eu/	LULC	Raster	10 m
Google Earth image	Google Earth Pro and field survey	Landslide inventory	Vector/polygon	-
Humanitarian data exchange	Downloaded from https://data.humdata.org	–Road -Study boundary	Vector/polyline Vector/polygon	-

CHAPTER V

DATA COLLECTION, PROCESSING AND ANALYSIS

5.1 Inventory Mapping

To precisely identify and record landslide-prone areas, an inventory map is crucial (Fig. 5.1). The existing landslide history serves as an essential component in determining hazard-prone areas in landslide mapping. Collecting data about past landslide events is essential for predicting future occurrences, as it provides insight into the causal factors that may trigger or reactivate landslides. On-site investigations were conducted to determine landslide scars, existing landslides, and pertinent features related to landslides. The magnitude, distribution, type, and location of landslides were accurately documented in the field notebook. For inventory mapping, 31 GPS points were collected through on-site investigations and analysis of images from Google Earth (Table. 5.1). From the total landslide inventory points, 70% (22 points) were utilized as training data, and the remaining 30% (9 points) were used as testing data to confirm the model's success and prediction rate. The verifying and testing data were randomly divided in ArcGIS selection by location. All the training point data were transformed into polygons. Subsequently, the polygons were rasterized using the polygon–to–raster conversion tool in a GIS environment. The data were primarily collected in the Geographic coordinate system WGS 1984 and the projection was Adindan UTM zone 37 N. The rasterized landslides were resampled to a similar pixel size along with other parameters.

Table 5.1: Landslide manifestation points.

S/N	Site name	Northing	Easting	Elevation (m)	Type
1	Aromba	11.4865	39.62244	1615	Gully erosion
2	Grar genda	11.5064	39.610846	1802	Rotational slide
3	Grar genda	11.5083	39.610011	1830	Rotational slide
4	Dembot	11.524	39.60388	2067	Rock fall
5	Limo	11.5011	39.663238	1748	Debris slide
6	Limo	11.5031	39.663783	1832	Debris slide

7	Qina amba	11.5039	39.580134	2255	Debris slide
8	Qina amba	11.504	39.578603	2326	Debris slide
9	Qina amba	11.4921	39.567338	2512	Debris slide
10	Robit	11.4779	39.570382	2054	Rock fall
11	Robit	11.476	39.584941	1827	Debris slide
12	Qina amba	11.5023	39.576391	2403	Debris slide
13	Qina amba	11.5058	39.571453	2712	Debris slide
14	Denugela	11.5054	39.613517	1836	Rock slide
15	Qina amba	11.4994	39.580888	2217	Debris slide
16	Robit	11.4785	39.563836	2195	Debris slide
17	Robit	11.4755	39.559325	2276	Debris slide
18	Dembot	11.5248	39.603715	2021	Rock fall
19	Melakie	11.513	39.596632	2016	Debris slide
20	Melakie	11.5147	39.593285	2077	Debris slide
21	Wuchale	11.5187	39.603234	2009	Debris slide
22	Wuchale	11.5195	39.602063	2087	Debris slide
23	Qina amba	11.5057	39.587372	2176	Debris slide
24	Dembot	11.5219	39.592764	2255	Rock fall
25	Robit	11.4857	39.56849	2064	Debris slide
26	Qina amba	11.4929	39.582656	2057	Debris slide
27	Robit	11.4488	39.570625	2485	Debris slide
28	Robit	11.4555	39.568793	2203	Debris slide
29	Robit	11.4567	39.567555	2277	Debris slide
30	Robit	11.4654	39.567428	2418	Debris slide
31	Qina amba	11.5	39.565994	2840	Debris slide

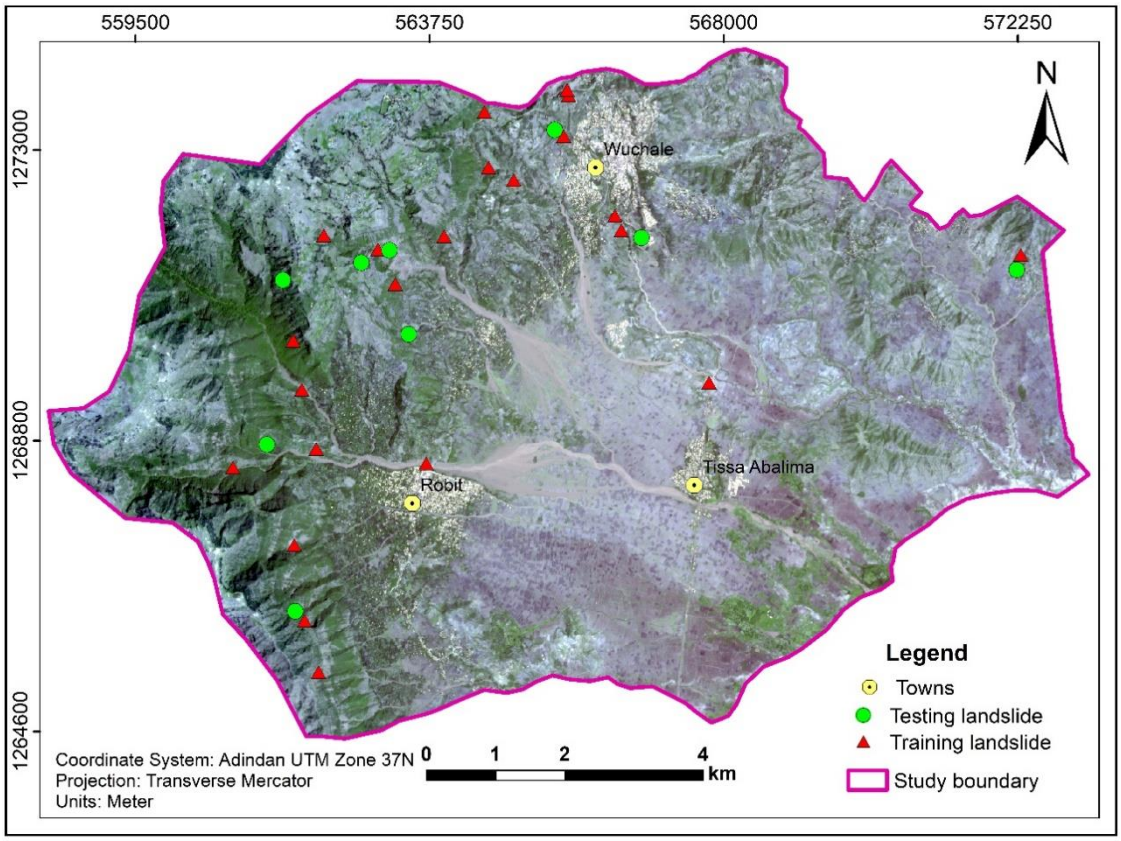

Figure 5.1: Landslide inventory map of Wuchale area.

5.2 Causing factors

Various natural and man-made variables have the potential to cause landslides (Bekele Abebe et al., 2010). To evaluate and map landslide susceptibility in the Wuchale area slope, aspect, elevation, LULC, proximity to a stream, and slope materials were analyzed. These variables were chosen based on the area's topography, geology, and landslide type. The comparative weight of every factor was analyzed and computed based on density ratio analysis in a GIS environment. All factor maps were prepared with uniform resolution and later the vector data was rasterized to know the area covered with landslide. Through overlay analysis, the area's total pixel and landslide pixels were counted, and the frequency ratio and information value was computed.

5.2.1 Slope

The behavior, frequency, and features of landslides can be influenced by slope. It can influence the slope stability by combining with other factors like geology and hydrogeology. The angle of inclination of the slope can influence soil or rock strength, the water seepage, and the growth and

distribution of vegetation, all of which can ultimately impact slope stability. The greater the slope angle will leads the material undergo sliding (Matebie Meten et al., 2015). Increased slope angle leads to increased shear stress, which can overcome the material's shear strength, causing slope failure. Slope angle can influence the kind of landslide that occurs. In research area, debris slides commonly happen on steep slopes, and rotational slides are common on relatively gentle slopes. A slope was extracted from ALOS PALSAR DEM 12.5 m, which was downloaded from the Alaska satellite facility (ASF). The slope angle generated for the area ranges from 0-81°. It was reclassified into 5 classes depending on Jenks natural interval: 0–9°, 9–20°, 20–31°, 31–45°, and >45° (Fig. 5.2). During the field observation, most of the landslides were observed in steep slope areas where the rocks are highly weathered and fractured. The analysis results also confirmed that there is a high landslide density in the slope class >20^{o}, but the most susceptible class is found in the slope class >45^{o} followed by 31–45°, and 20–31°(Table 6.1).

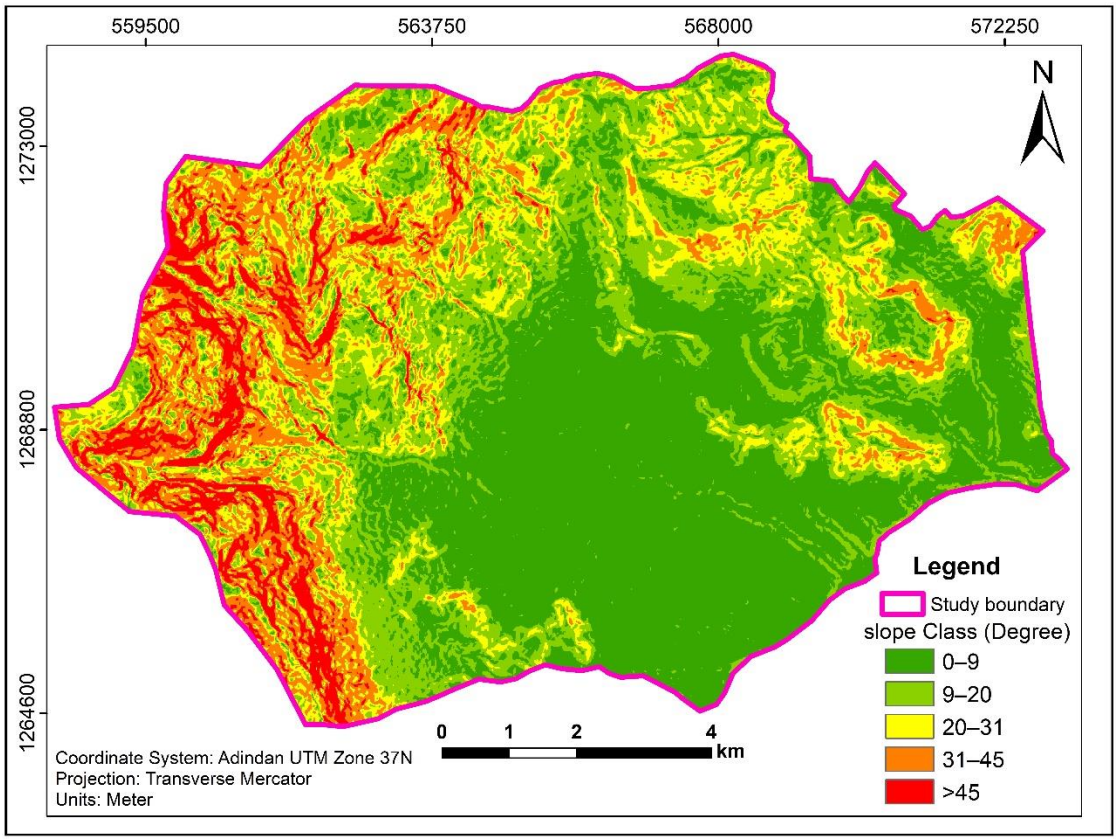

Figure 5.2: Slope map of the study area.

Table 5.3: Slope class.

S/N	Slope Class (Degree)	Area covered	
		Area (Km^2)	Area (%)
1	0–9°	39	39
2	9–20°	25	25
3	20–31°	17	17
4	31–45°	13	13
5	>45°	6	6
Total		100	100

5.2.2 Aspect

Aspect is affiliated with the direction that a slope is facing, and it can have an impact on the amount of sunlight and wind exposure that a slope receives. The aspect map was extracted from ALOS PALSAR DEM 12.5 m, obtained from the Alaska website. After downloading, the DEM was extracted by mask to a desired area of interest in the GIS environment to produce the aspect map. Aspect classes were reclassified based on natural breaks (Jenks) in the reclassify interface. The research area is divided into nine (9) distinct aspect classes viz: flat, north, south, northeast, east, southeast, southwest, northwest, and west (Fig. 5.3). The north and northeast-facing slopes inhabit a larger percentage of landslide coverage as well as higher values of FR and IV (Table 6.1). This may be because the slopes facing north and northeast receive a less amount of direct sunlight, resulting in cooler and moisture conditions. This favoring the occurrences of landslides due to saturation and weathering, particularly in weathered and fractured rocks.

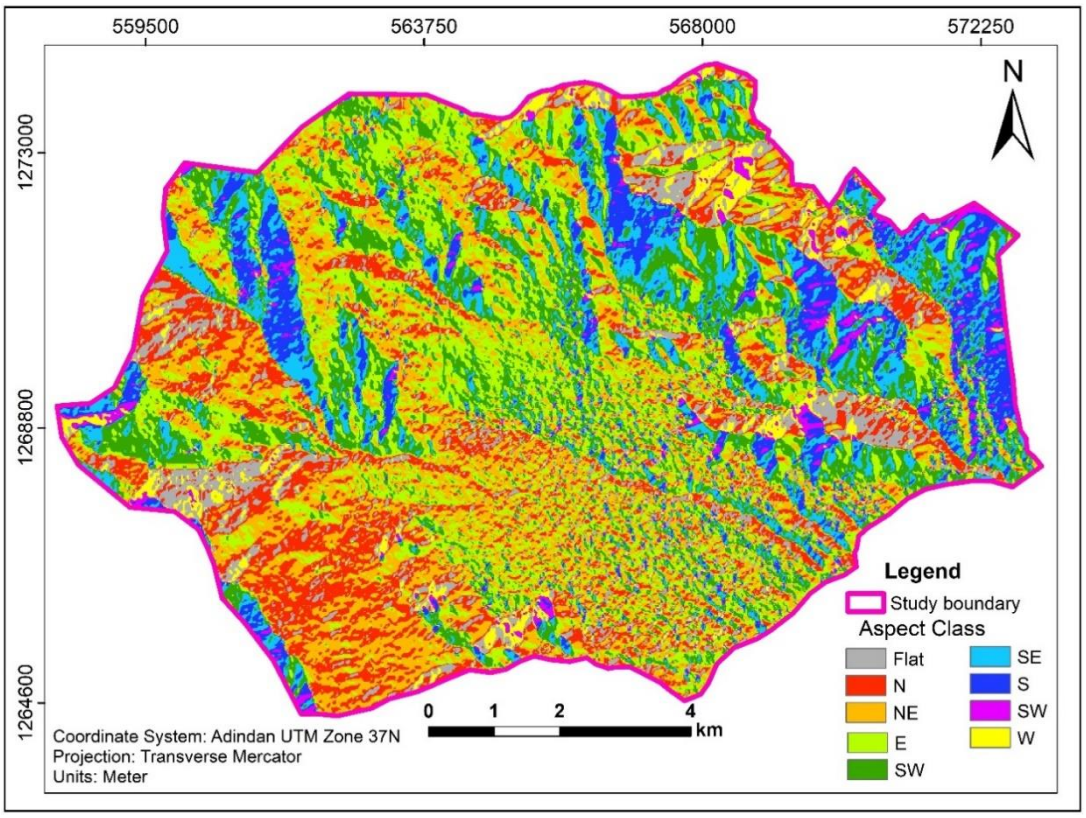

Figure 5.3: Aspect map of the study area.

Table 5.4: Aspect class

S/N	Aspect Classes	Area covered	
		Area (km^2)	Area (%)
1	Flat	10	10
2	N	16	16
3	NE	21	21
4	E	20	20
5	SE	15	15
6	S	10	10
7	SW	4	4
8	W	1	1
9	NW	3	3
Total		100	100

5.2.3 Elevation

Elevation is a factor that determine the slope stability. It influences several factors that contribute to landslides. The elevation map was sourced from the ALOS PALSAR DEM 12.5 m, obtained from the Alaska website. The elevation classes were accurately reclassified in the reclassify interface through Jenks natural interval. The area occupies a lowest of 1437 m and a highest of 3522 m in elevation. The elevation difference is about 2085 m, indicating high topographic variations in the area. As a conditioning factor, the elevation was reclassified into five classes viz; 1437–1747, 1747–2060, 2060–2459, 2459–2885, and 2885–3522 m (Fig. 5.4). High landslide occurrences were recorded within the height class of 2459–2885 m. Based on field observations, slightly elevated areas with vegetated to slightly vegetated regions and weak rock units exhibit a higher concentration of landslides.

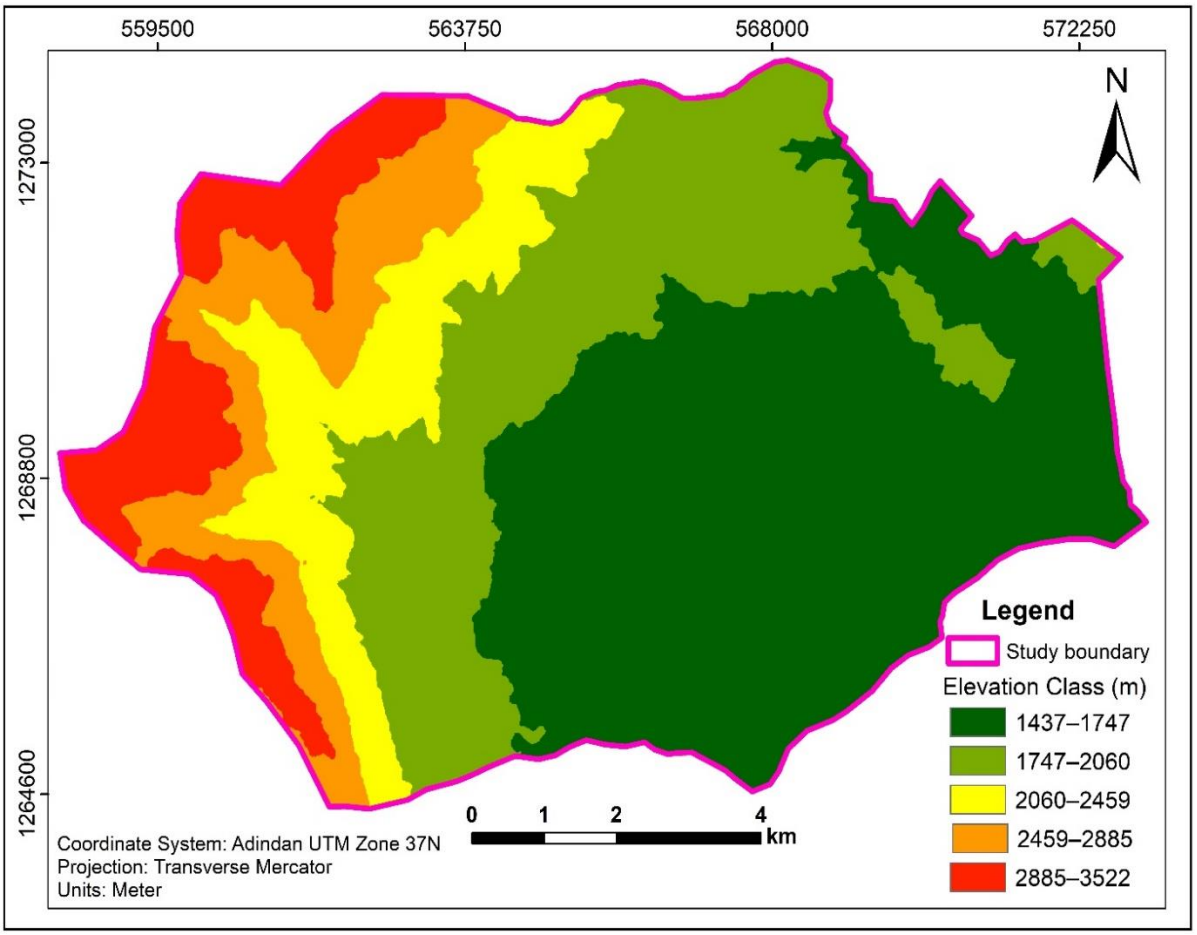

Figure 5.4: Elevation map of the study area.

Table 5.5: Elevation class.

S/N	Elevation Classes (m)	Area covered	
		Area (Km^2)	Area (%)
1	1437–1747	44	44
2	1747–2060	26	26
3	2060–2459	11	11
4	2459–2885	10	10
5	2885–3522	9	9
	Total	100	100

5.2.4 Distance to Streams

Streams are a vital element that can help us to identify landslides and erosional surfaces. Their presence indicates potential water flow pathways, and areas close to streams are more sensitive to erosion and degradation, which can increase the phenomenon of landslides. In this research, the stream data were extracted from ALOS PALSAR DEM 12.5 m resolution sourced from Alaska satellite facility. Operations including fill, flow accumulation, and flow direction were executed and later raster calculator were done in GIS environment. Subsequently, raster images were vectorized (polyline format) to derive stream order information. Using this stream order data as an input, Euclidean distance calculations were performed to get stream proximity. The output Euclidean distance stream raster was then reclassified using the reclassify tool. By understanding the relationship between stream networks and landslides, the stream proximity channel map was manually reclassified into five classes viz: 0–50, 50–100, 100–150, 150–200, and >200 m (Fig. 5.5). The threshold values of proximity to the stream map were determined by understanding the interaction between landslides and streams in the area, as well as literature. Similar classification were used by Thapa & Bhandari (2019). The primary basis for selecting this element was how landslides and streams interacted within the research region. The majority of the landslides particularly, in Qina Amba, Robit, and Aromba, are found in the vicinity of streams and rivers. As we move away from the streams, the density of landslides decreases. A higher correlation between landslide and stream distances is observed near the stream.

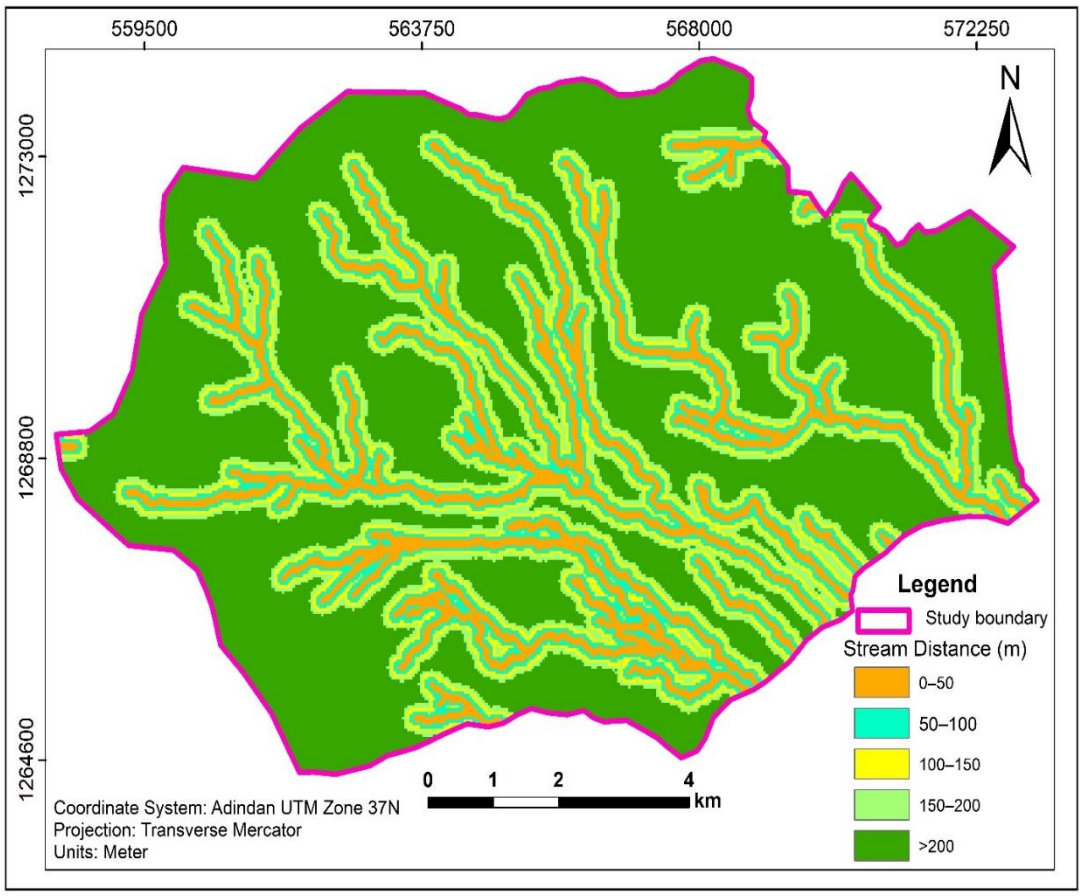

Figure 5.5: Stream proximity map of the study area.

Table 5.6: Distance to stream class.

		Area covered	
S/N	Distance from stream (m)	Area (km^2)	Area (%)
1	0–50	13	13
2	50–100	11	11
3	100–150	10	10
4	150–200	10	10
5	>200	56	56
	Total	100	100

5.2.5 Slope material

Slope material for this study was prepared by integrating the data gathered from the Geological Survey of Ethiopia (GSE) and extensive field surveys at 1:50,000 scale (Fig. 5.6). The rock and

soil materials were systematically classified based on their degree of weathering, composition, size, and strength. Accordingly, the slope materials in the area are classified into massive basaltic rocks, rhyolite rocks, unwelded tuff, weathered and fractured basalts, alluvial, and colluvial deposits. Colluvial soils take higher proportions in the area (37%), followed by fractured and weathered basalts (23%), massive basalt (21%), rhyolite (11%), alluvial soil (6%), and unwelded tuff (2%) (Table. 5.7). Landslides occur in all the lithological units in the study region, with scale, density, and degree varying based on rock type, strength, and weathering. Fractured and weathered basalts are highly susceptible to landslides during the field investigations. These basalts are characterized by intense weathering, fracturing, and jointing compared to other lithological units in the study area.

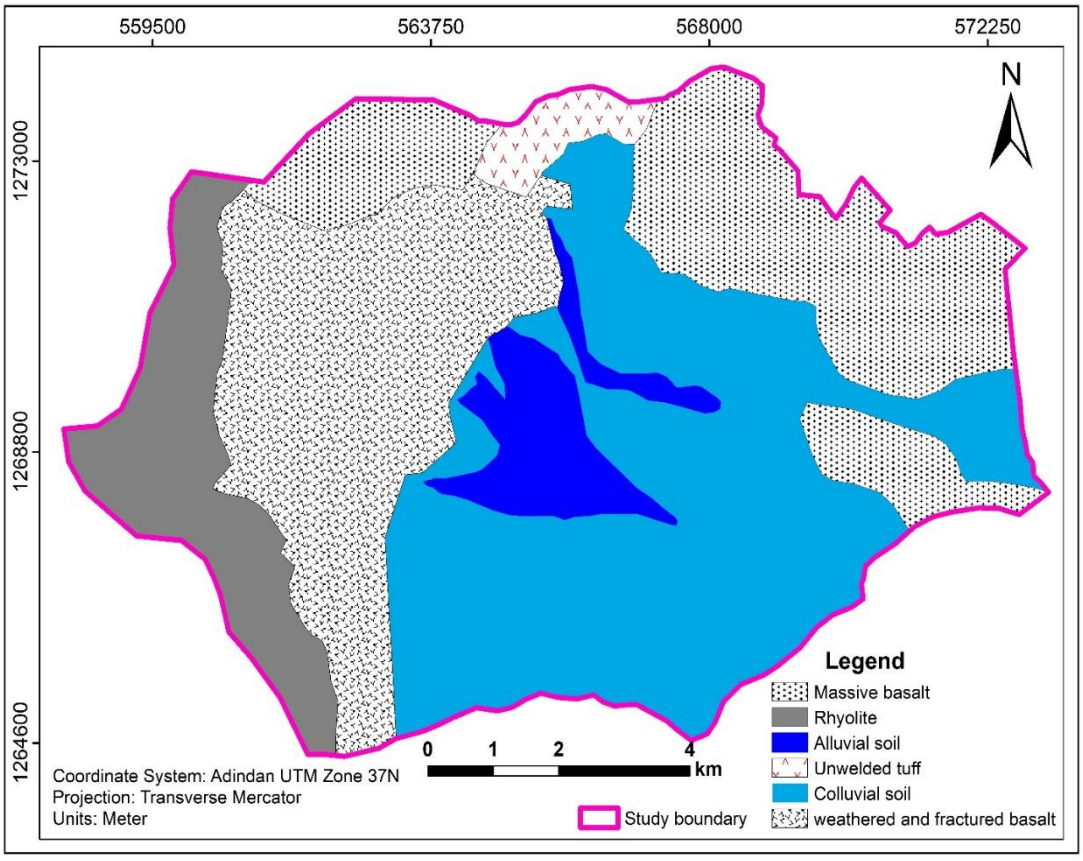

Figure 5.6: Slope material map of the area.

Table 5.7: Slope material class.

		Area covered	
S/N	Slope material Classes	Area (Km^2)	Area (%)
1	Massive Basalt	21	21
2	Rhyolite	11	11
3	Fractured and Weathered basalt	23	23
4	Unwelded Tuff	2	2
5	Alluvial soils	6	6
6	Colluvial soils	37	37
	Total	100	100

5.2.6 Land use–land cover/LULC

A high–resolution Sentinel–2A image was downloaded from Copernicus at 10 m resolution, and the spectral bands B2, B3, B4, and B8 were combined to make a false-color composite for better interpretation of surface features and classification. ArcGIS 10.4 was utilized for combining these bands, and later supervised classifications were done. For supervised classifications, several training data points were fed to the model from various classes of features. The raster LULC map was resampled to similar pixel sizes with other parameters. Subsequently, the area was categorized into six LULC classes: agricultural land, bare land, built–up, river, sparse vegetation, and vegetated area (Fig. 5.7). Most researchers suggested that there is a limited chance of landslide occurrence in vegetated areas. Through its roots, vegetation can enhance slope stability and soil erosion because the roots uptake more water and bind the soil together, thus reducing the water content in the soil. Field investigations revealed high landslide concentration in vegetated and slightly vegetated areas, possibility due to plant species, root characteristics, human activities, soil type, slope morphology, and geology.

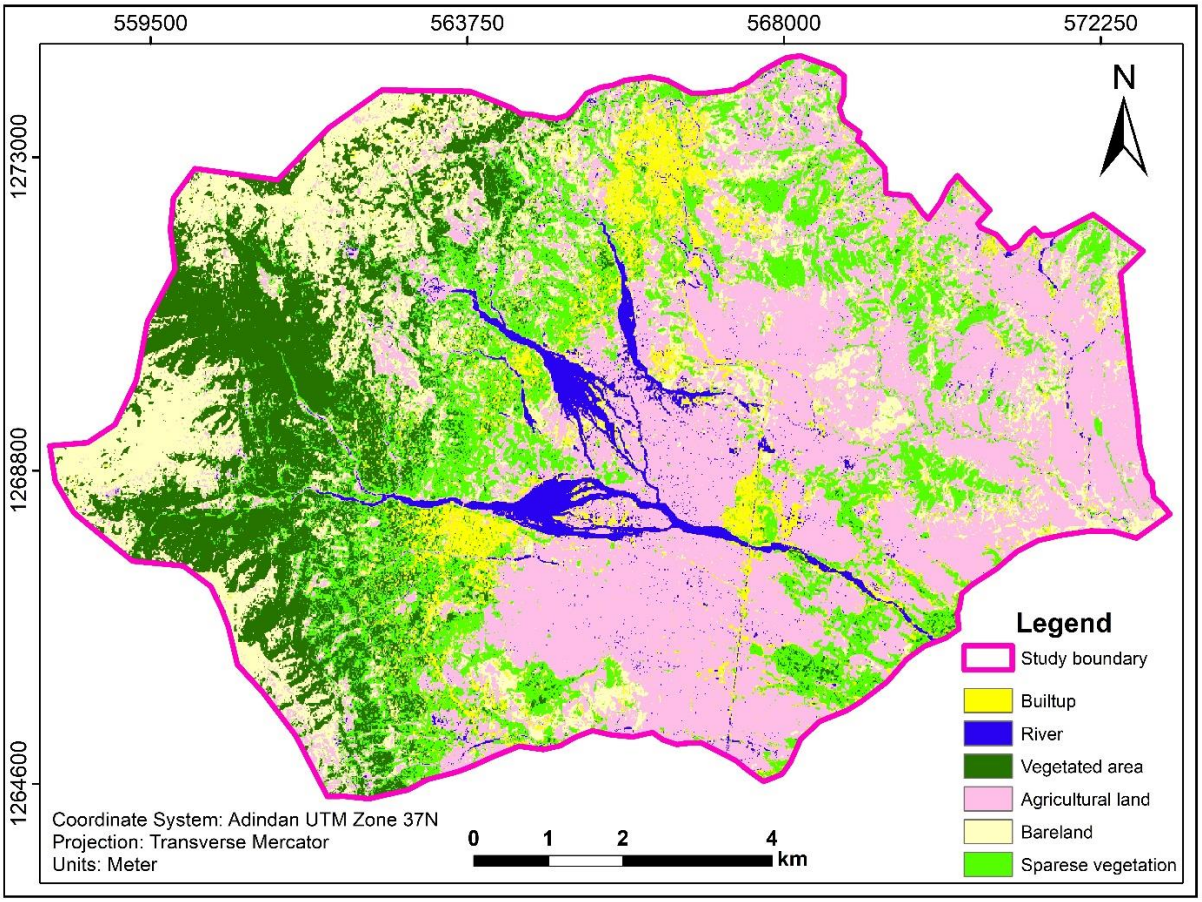

Figure 5.7: LULC map of Wuchale area

Table 5.8: Land use–land cover class.

S/N	Land use/Land cover	Area covered	
		Area (Km^2)	Area (%)
1	Built–up	7	7
2	River	3	3
3	Vegetated area	15	15
4	Agricultural land	38	38
5	Bare land	19	19
6	Sparse Vegetation	18	18
	Total	100	100

Table 5.9: Description of land use-land cover classes.

S/N	Class	FAO (2005)	Description (in this study)
1	Built-up	Areas consists of urban areas, industrial areas, and infrastructure areas.	Areas with human-made structures including houses, buildings, and villages.
2	River	Areas comprised of inland waters (lakes, rivers, and reservoirs)	Areas containing predominantly waters. But in this study, the water does not flow continuously year-round.
3	Vegetated area	Areas comprised of forests grass lands, and shrubs.	Areas covered with trees, bushes, shrubs, and grass.
4	Agricultural land	Areas consists of arable land, permanent crops, and pastures.	Areas comprise human-planted seasonal crops such as corn, wheat, maize, beans, peas, and other.
5	Bare land	Areas consists of natural land (areas with little or no vegetation, such as deserts, beaches, and rocky outcrops) and artificial bare land (Man-made areas with little or no vegetation, such as quarries, construction sites, and waste disposal sites.)	Areas covered with rocks or soils without any cultivation or vegetation.
6	Sparse vegetation	Areas where plant cover is limited, with a low density of plants spread across the landscape.	Areas covered with sparsely distribution of vegetation. The plants are found widely spaced in the area.

5.3 Landslide susceptibility mapping

Once we have collected the data regarding the failure mechanisms, conditioning factors, and the extent of damage experienced, the next crucial steps involve delineating the areas into different susceptibility classes. This is commonly known as landslide susceptibility mapping (Anbalagan, 1992). This can be done by analyzing different landslide conditioning factors that were contributing to the occurrence of existing landslides in a particular area. In this study, a statistical bivariate frequency ratio and information value were applied to produce the final susceptibility map. Aspect, slope, elevation, stream distance, LULC, and lithology were important parameters selected to prepare the map. Primarily, the landslide inventory map and all factor maps were prepared and resampled to get similar resolutions. Later, they were rasterized into raster datasets to count the existence of landslide pixels in each subclass of each parameter. For this process, Arc GIS 10.4 was utilized. After the pixels were properly counted, the values of FR and IV models of every parameter was computed in Excel using Eq. 1 and Eq. 3 respectively. Finally, LSI was calculated in the GIS environment utilizing the raster calculator tool as per Eq. 3&7, and the final map was produced for the two models (Fig. 6.3).

5.3.1 Frequency ratio model (FR)

Frequency ratio is among the statistical techniques used to quantify the connection between the incidence of landslides and different factors or causes that lead to their initiation (Lee & Pradhan, 2007). It assists in determining an area's landslide susceptibility based on how frequently landslides occur in response to these parameters. This approach examines the relationships between causing factors and the distribution of past landslides. Landslide inventories and factor maps are required to produce the landslide susceptibility map of a particular area employing the frequency ratio model (Thapa & Bhandari, 2019). It helps to identify the most probable conditioning factor for the occurrence of a landslide in a particular area. As stated by Lee & Pradhan (2007), a frequency ratio value of 1 indicates an average association, a value >1 indicates a higher association, and a value <1 indicates a weaker association with the landslides.

The frequency ratio can be computed as the likelihood of a landslide event occurring within a particular class of a conditioning element divided by the likelihood of a landslide event occurring throughout the study area.

$$FR = \frac{N_i L_x / N}{N_i P_x / NI} = \frac{\%\ of\ landslide\ pixels\ in\ each\ \ subclass}{\%\ of\ total\ pixes\ in\ the\ subclass\ of\ a\ factor} \quad (1)$$

where $N_i L_x$ represents the number of landslide pixels in every factor class, N stands for the overall count of landslide pixels in the study area, $N_i P_x$ is the number of pixels in each conditioning factor class, and NI stands for total numbers of pixels of the study area.

After calculating the FR of each subclass of the conditioning class, we can calculate the Landslide Susceptibility Index (LSI) to provide the weighted maps:

$$LSI = \sum_{i=1}^{n} FR_{ij} \quad (2)$$

where LSI stands for landslide susceptibility index and FR_{ij} denotes the frequency ratio value of the "j" class of factor "i".

5.3.2 Information value method (IV)

As cited in Sarkar et al. (2013), the IV model was initially presented by Yin & Yan (1988) and subsequently refined by Van Westen (1993). In information value, the weight of individual factor classes can be established by understanding the relative significance of contributing factors and landslides. The IV model is a bivariate statistical approach that utilizes correlations between landslide incidence and associated parameters to predict and analyze landslides spatially, and it can be quantified using (Eq. 3) (Mandal & Mandal, 2017).

$$w_i = \ln \frac{N_{pix}(xi)/N_{pix}(Ni)}{\Sigma N_{pix}\,(xi)/\Sigma N_{pix}\,(Ni)} \quad (3)$$

where w_i is the factor class weight, $N_{pix}(xi)$ is the number of pixels of landslide within class i, $N_{pix}(Ni)$ is the number pixel of class i, $\Sigma N_{pix}\,(xi)$ is the total number of landslide pixel in the study area, and $\Sigma N_{pix}\,(Ni)$ is the total pixel number of the study area.

In another way, IV is also computed as:

$$IV = ln \frac{Conditional\ probability}{prior\ probability} \quad (4)$$

$$Conditional\ probability = \frac{number\ of\ pixels\ of\ landslides\ with\ in\ each\ subclass}{number\ of\ pixel\ of\ the\ study\ area\ within\ that\ subclass} \quad (5)$$

$$Prior\ probability = \frac{Total\ number\ of\ pixel\ of\ landslides\ with\ in\ the\ factor\ class}{Total\ number\ of\ pixel\ of\ the\ study\ area\ within\ the\ factor\ class} \quad (6)$$

The natural logarithm is employed to calculate negative and positive values when the density of the landslide is lower and higher than usual respectively (Sarkar et al., 2013). Therefore, a positive weighting factor reveals there is a positive correlation between the factor class and landslide occurrence, while a negative value indicates a negative relationship between landslides and the factor class.

From the values obtained using Eq. 3 or 4, LSM can be generated by totaling the IV values of every contributing factor in ArcGIS using a raster calculator as per Eq.7.

$$LSI = \sum_{i=1}^{n} IV_{ij} \quad (7)$$

where LSI stands for landslide susceptibility index and IV_{ij} denotes the IV value of the "j" class of factor "i".

Given the above equations, the LSI of the present study was computed as:

$$LSI = Slope_{wi} + Elevation_{wi} + Aspect_{wi} + LULC_{wi} + Distance\ to\ stream_{wi} + Lithology_{wi}$$

where w_i is the factor class weight, and slope, elevation, aspect, LULC, stream proximity, and lithology were the conditioning parameters considered in this study.

CHAPTER VI

RESULTS AND DISCUSSION

6.1 Results

6.1.1 Landslide inventory

Landslide inventory was executed by employing an integrated on-site investigation and Google Earth Images. In total 31 landslide GPS points were collected throughout the study region. Out of 31 landslides, 9 were found along the stream paths of Qina amba, 9 were collected from Robit, 3 landslides from Dembot, 2 landslides from Grar Genda, 2 from Wuchale, 2 from Melakie, and the remaining 4 landslides were recorded from Limo, Denugela, and Aromba sites (Table 5.1). From the total study area of 100 km^2 (Fig. 3.1), 3.9 km^2 is covered by a landslide. The geographic dispersion of landslides in the area is shown in Fig.5.1. Most of the landslides were found in the northwestern part of Wuchale town.

6.1.2 Conditioning factors

6.1.2.1 Slope

The area's slope angle were grouped into five classes (Fig. 5.2). The area they covered is clearly presented in Table 5.3. Table 6.1 illustrates that as the slope angle becomes steeper the FR and IV value also increased. The slope class >20° has a frequency ratio value greater than one (1). Conversely, the gentle slope classes have a FR value of less than one (1). In the same manner, the information value result also shows that there is a higher value in the steeper slope classes and lower values in the gentle slope classes (Table 6.1). Therefore, the results indicate a positive correlation between landslides and slope class of >20° for both frequency ratio and information value. However, there is a negative correlation between landslides and the remaining slope classes (<20°). Therefore, based on this scenario the slope class >20° is more prone to landslides, while slope classes <20° are more stable.

6.1.2.2 Aspect

The aspect class of the study area was categorized into nine (9) classes (Fig. 5.3). The area they covered is clearly described in Table 5.4. The highest values of FR and IV is observed in the aspect class north and northeast. Based on the results indicated in Table 6.1, landslide events are more

likely to occur within these classes of aspects. In both frequency ratio and information value, the aspect class north is more prone to landslide followed by northeast. The remaining aspect classes have a negative association with landslides.

6.1.2.3 Elevation

The elevation class of the study area is grouped into five classes (Fig. 5.4). About 44% of the research area is covered by class 1437–1747 m, 26% is covered by 1747–2060 m, 11% is covered by 2060–2459 m, 10% covered by 2459–2885 m, and the remaining 9% falls under the slope class 2885–3522 m (Table 5.5). A high FR (5.021) and IV (1.614) values are observed in the elevation class 2060–2459 m (Table 6.1). The result reveals that the elevation class 2060–2459 m is more likely susceptible to landslides followed by the 2459–2885m class.

6.1.2.4 Distance to stream

This is an important parameter to delineate landslide-prone areas in the research area. During the fieldwork, most of the active landslides were observed along the stream and river pathways. Some of the rivers dissected the area and formed a deep gorge, particularly in the Aromba site. The distance to stream map of the study was grouped into five classes (Fig. 5.5). The proportion of each stream distance class is clearly shown in (Table 5.6). Stream distances from 0–50 m have higher FR (1.575) and IV (0.454) values, succeeding by stream distances of 50–100 m with a value of 1.308 and 0.268 FR and IV respectively (Table 6.1). Therefore, this value shows that the area close to the streams is more prone to landslides and there is a strong association between landslide and stream networks.

6.1.2.5 Slope material

Lithology is the most crucial influencing factor in landslide events. The more strengthened rocks have a high resistance to weathering and consequently they are more stable. Rocks that are fragile, fractured, foliated, and sheared are more likely to have landslides. During the field survey, most of the landslides were recorded from weathered and fractured basalt units. The analysis result also confirmed that there is a higher value of FR and IV within this class (Table 6.1). The FR and IV value results demonstrate that there is a positive correlation between landslides and fractured and weathered basalts with a value of 3.117 and 1.137 respectively.

6.1.2.6 Land use–land cover

The study area was categorized into six LULC classes after an extensive field observation and supervised classifications of Sentinel 2A images with a remarkable 10 m resolution (Fig. 5.7). Agricultural land takes the higher proportion (38%), bare land (19%), sparse vegetation (18%), vegetated area (15%), Built–up (7%), and river covered (3%) of the study area (Table 5.8). The landslide overlay analysis result reveals that 34.014% of the existing landslide falls under vegetated area, 27.674% in sparse vegetation class, 18.392% in bare land, 15.901% in agricultural land, 2.467% in the river, and 1.551% in built-up area (Table 6.1).

Table 6.1: Landslide conditioning factors with their respective FR and IV value.

Parameter	Classes	class pixel	% of the class pixel	landslide pixel	% of landslide pixel	FR	*IV*
Slope	0-9	256948	40.380	712	3.494	0.087	-2.447
	9-20	145194	22.818	2810	13.788	0.604	-0.504
	20-31	113882	17.897	5310	26.055	1.456	0.376
	31-45	81554	12.816	7271	35.677	2.784	1.024
	>45	38745	6.089	4277	20.986	3.447	1.237
	Total	**636323**	**100**	**20380**	**100**	**8.377**	**-0.314**
Aspect	Flat	51317	8.065	1191	5.844	0.725	-0.322
	N	91059	14.310	5673	27.836	1.945	0.665
	NE	122620	19.270	5161	25.324	1.314	0.273
	E	123367	19.387	3415	16.757	0.864	-0.146
	SE	102450	16.100	2009	9.858	0.612	-0.491
	S	64154	10.082	1729	8.484	0.841	-0.173
	SW	48770	7.664	875	4.293	0.560	-0.579
	W	13583	2.135	61	0.299	0.140	-1.965
	NW	19003	2.986	266	1.305	0.437	-0.828
	Total	**636323**	**100**	**20380**	**100**	**7.439**	**-3.564**
Proximity to stream	0-50	82743	13.003	4173	20.476	1.575	0.454
	50-100	70297	11.047	2944	14.446	1.308	0.268

	100-150	60171	9.456	2112	10.363	1.096	0.092
	150-200	57021	8.961	1598	7.841	0.875	-0.134
	>200	366091	57.532	9553	46.874	0.815	-0.205
	Total	**636323**	**100**	**20380**	**100**	**5.668**	**0.475**
LULC	Built-up	42435	6.669	382	1.874	0.281	-1.269
	River	21533	3.384	581	2.851	0.842	-0.171
	Vegetated area	96566	15.176	6327	31.045	2.046	0.716
	Agricultural land	236525	37.171	3386	16.614	0.447	-0.805
	Bare land	123668	19.435	3777	18.533	0.954	-0.048
	Sparse Vegetation	115590	18.165	5927	29.082	1.601	0.471
	Total	**636323**	**100**	**20380**	**100**	**6.171**	**-1.107**
Elevation	1437-1747	282912	44.460	145	0.711	0.016	-4.135
	1747-2060	160074	25.156	4318	21.187	0.842	-0.172
	2060-2459	71221	11.193	11454	56.202	5.021	1.614
	2459-2885	62922	9.888	4460	21.884	2.213	0.794
	2885-3522	59194	9.303	3	0.015	0.002	-6.449
	Total	**636323**	**100**	**20380**	**100**	**8.094**	**-8.347**
Slope materials	Massive Basalts	136947	21.522	319	1.565	0.073	-2.621
	Rhyolite	69332	10.896	3450	16.928	1.554	0.441
	Alluvial Soils	37038	5.821	144	0.707	0.121	-2.109
	Unwelded tuff	13486	2.119	1148	5.633	2.658	0.978
	Colluvial Soil	235235	36.968	913	4.480	0.121	-2.110
	Fractured basalt	144285	22.675	14406	70.687	3.117	1.137
	Total	**636323**	**100**	**20380**	**100**	**7.644**	**-4.285**

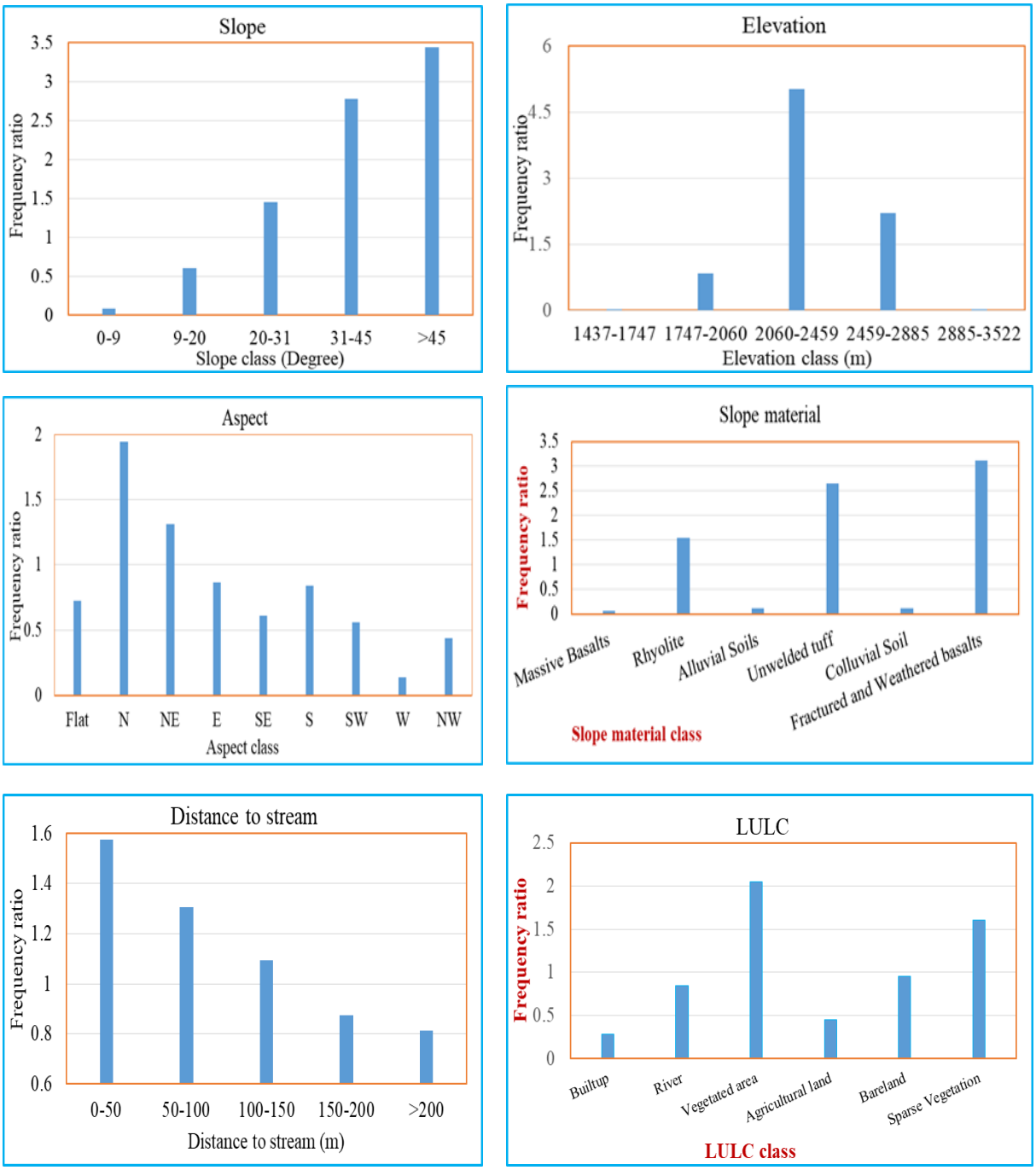

Figure 6.1: FR values of factor classes.

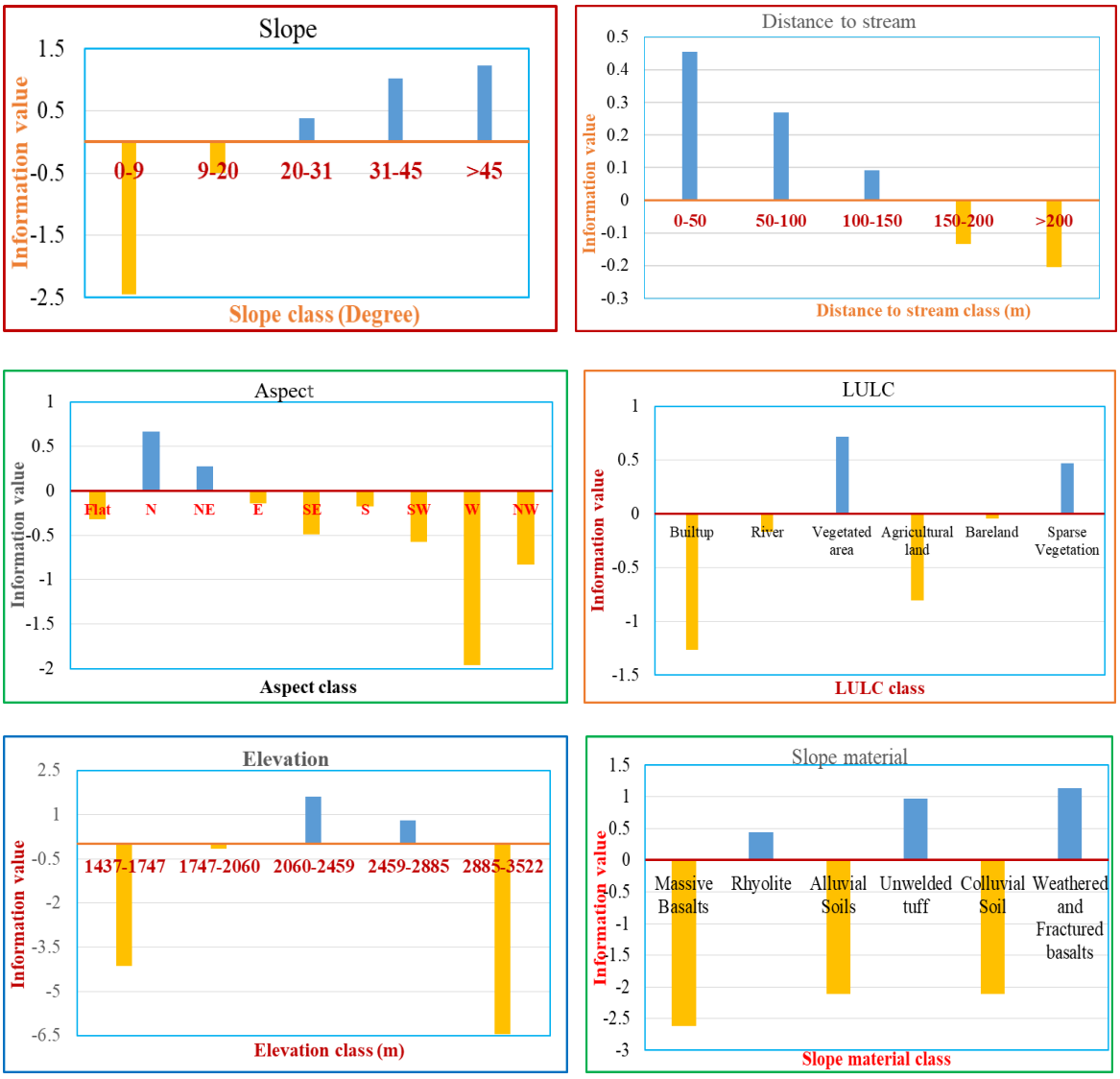

Figure 6.2: IV values of each factor class.

Table 6.2: Prominent class from each factor.

S/N	Parameters	Class	FR	IV
1	Slope	>45°	3.447	1.237
2	Aspect	North	1.945	0.665
3	Elevation	2060-2459 m	5.021	1.614
4	Distance to stream	0-50 m	1.575	0.454
5	LULC	Vegetated area	2.046	0.716
6	Slope material	Fractured basalt	3.117	1.137

6.1.3 Landslide susceptibility mapping

To create landslide susceptibility map, information value and frequency ratio methods were executed in this study. The type and distribution of the landslides were initially determined through a comprehensive field survey and later verified in GIS. The comparative importance of every casual factor was evaluated properly and ratings were given based on their contribution to the landslide occurrence. The frequency ratio and information value was computed using Eq. 1 and 3. After the FR and IV had been calculated, the factor maps were assigned the new values by using look up tool in GIS environment. Finally, each factors were summed up using raster calculator and the susceptibility maps are generated. The higher pixel values have a higher probability of landslide susceptibility and conversely the lower susceptibility results in lower pixel size. Therefore, the study area is divided into five susceptible areas based on the natural break (Jenks) viz; very high, high, moderate, low, and very low susceptibility classes (Fig. 6.3). This classification was performed by considering the landslide susceptibility index ranges presented in columns 3 of Table 6.3 and 6.4.

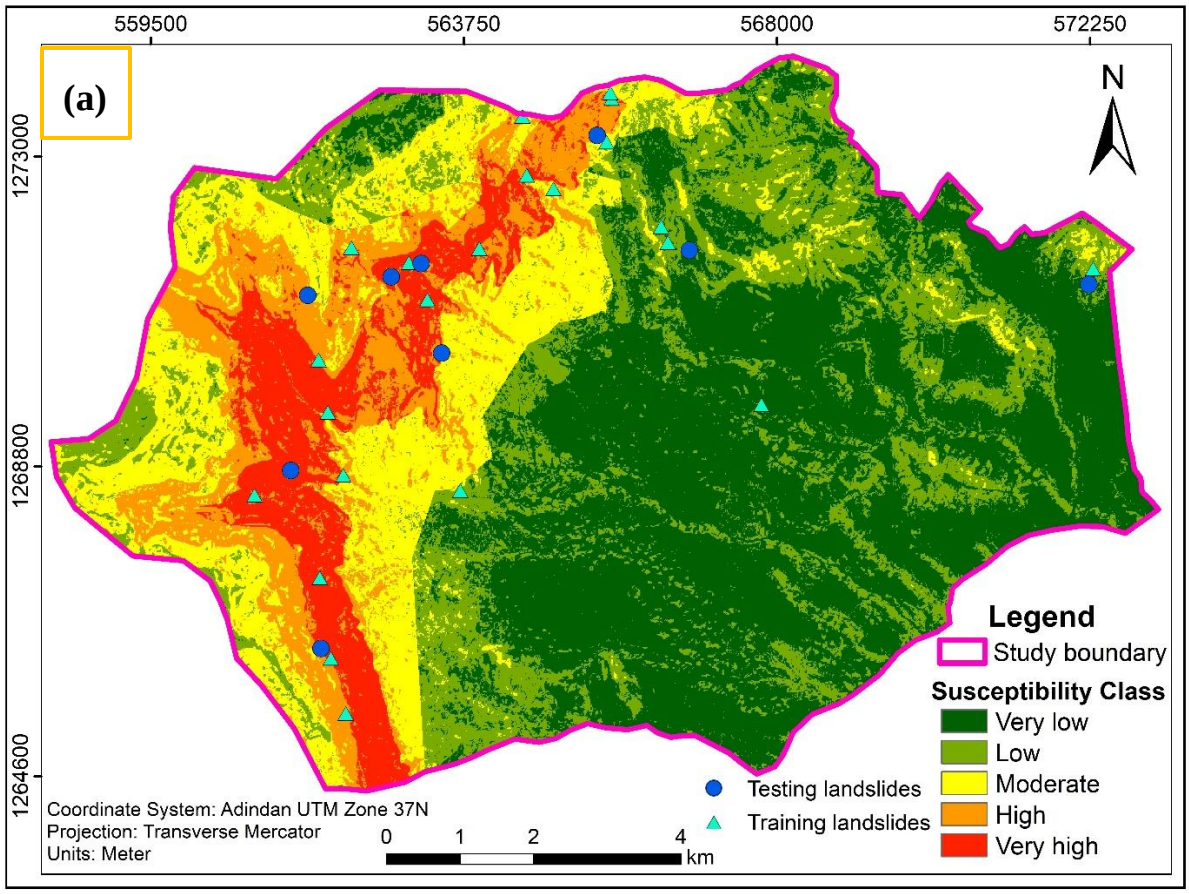

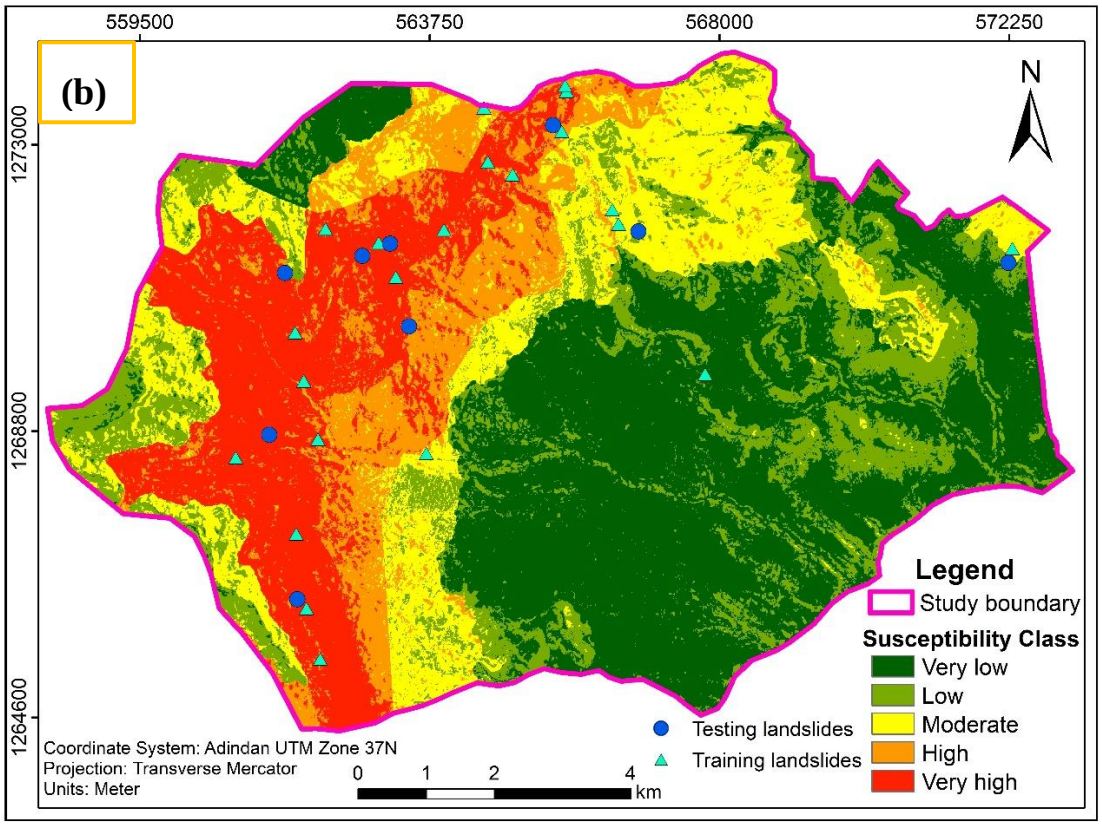

Figure 6.3: Landslide susceptibility map using FR model (a) and IV model (b).

Table 6.3: Landslide susceptibility index (LSI) of frequency ratio model.

		Frequency ratio (FR)			
S/N	Susceptibility Class	LSI	No of pixels	Area (km^2)	Area (%)
1	Very high	12.64-17.15	51891	9	9
2	High	9.42-12.64	69587	11	11
3	Moderate	6.27-9.42	110216	17	17
4	Low	3.8-6.27	146798	23	23
5	Very low	1.39-3.8	257831	40	40
	Total		636323	100	100

Table 6.4: Landslide susceptibility index (LSI) of information value model.

Information value (IV)					
S/N	Susceptibility Class	LSI	No of pixels	Area (km^2)	Area (%)
1	Very high	1.74-5.82	114636	18	18
2	High	-1.75-1.74	76448	12	12
3	Moderate	-5.25- -1.75	107173	17	17
4	Low	-8.19- -5.25	116053	18	18
5	Very low	-14.95- -8.19	222013	35	35
		Total	636323	100	100

6.1.4 Validation

Once the landslide-related parameters are identified, and evaluated, and the final map has been produced the next step should be model validation. Validation can be performed by qualitative (simple overlay) or quantitative (constructing cumulative curves) comparison (Remondo et al., 2003). Some researchers such as Filagot Mengistu et al. (2019) and Sendu Demessie & Raghuvanshi (2019) used a simple overlay method to check the model efficiency. The authors have overlaid the landslide inventory on the landslide susceptibility map. Subsequently, they counted the number of landslides that fall on each susceptible class. Conversely, other scholars used quantitative way of validation to check the model's efficiency. For this operation, they were used training and validating data. The training data were fed to the model to construct the susceptibility map, while the validating data were not used in the model construction and were utilized for validation. As stated by Yesilnacar & Topal (2005), the area under the ROC curve is among the mathematical techniques utilized by many researchers to check the model prediction ability. The authors noted that the AUC value varies from 0.5 to 1. In case the AUC value is 0.9–1, 0.8–0.9, 0.7–0.8, 0.6–0.7, and 0.5–0.6 the model has an excellent, very good, good, average, and satisfactory performance respectively (Azemeraw Wubalem, 2020). While the model has a poor performance when the AUC value is less than 0.5 (Yesilnacar & Topal, 2005). In the present

study, the area under the ROC curve was utilized to characterize the quality of the predictive ability of the models. The landslide point data were randomly divided as 70% (22 points) for training data and 30% (9 points) serves as testing data in ArcGIS by keeping their geographic distribution. The success and prediction rates were determined based on the training data and testing data. The success rate was established from the comparison between the final susceptibility map and training data employed in the model. It aids in assessing how accurately the produced susceptibility map has characterized the regions of existing landslides (Remondo et al., 2003). The prediction rates were determined depending on the susceptibility map and testing dataset. ArcSDM tools were utilized to generate the success and prediction rate curve in the GIS environment. The validation result shows that the information value model has a success rate of 0.786 (78.6%) (Fig. 6.4 a) and a prediction rate of 0.83 (83%) (Fig. 6.4 b). Similarly, Fig. 6.4 c & d shows the success rate (0.78) and prediction rate (0.828) of the FR model respectively. Although there is little difference in AUC values of the prediction rate in FR and IV, both models are relevant for landslide susceptibility mapping. Depending on the results, the model selected for this study successfully predicted the landslide susceptibility classes.

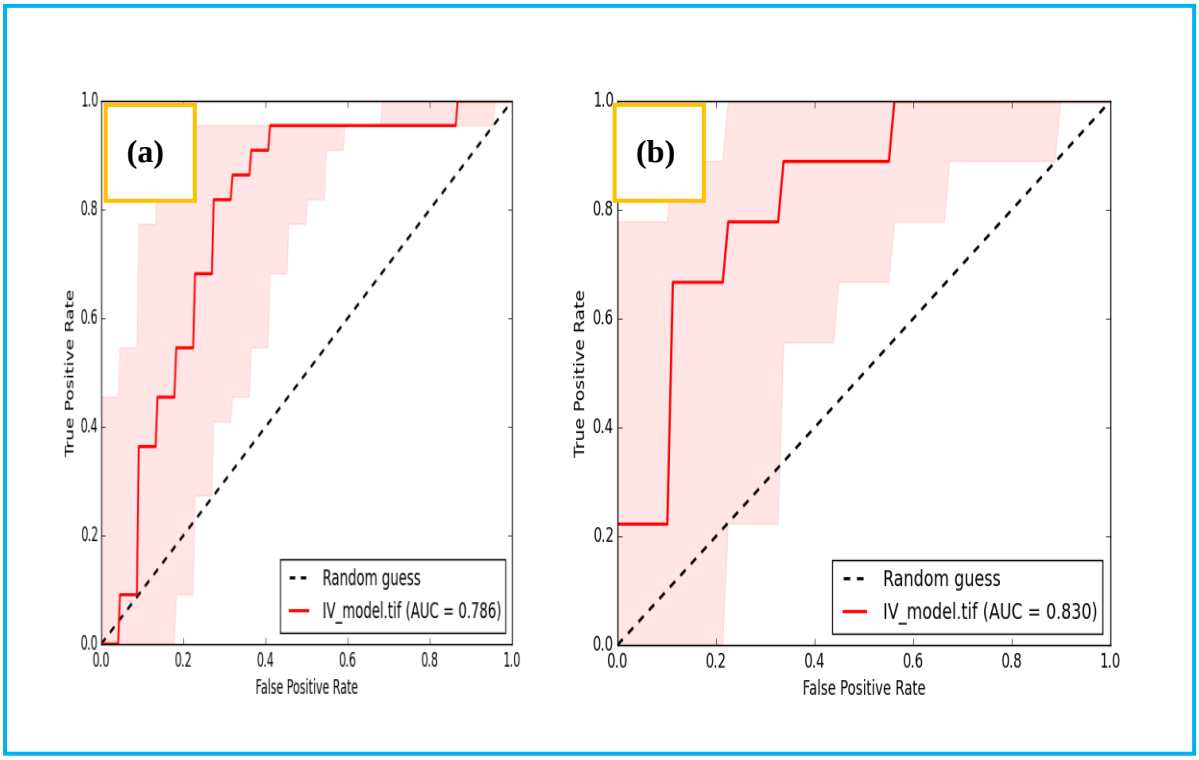

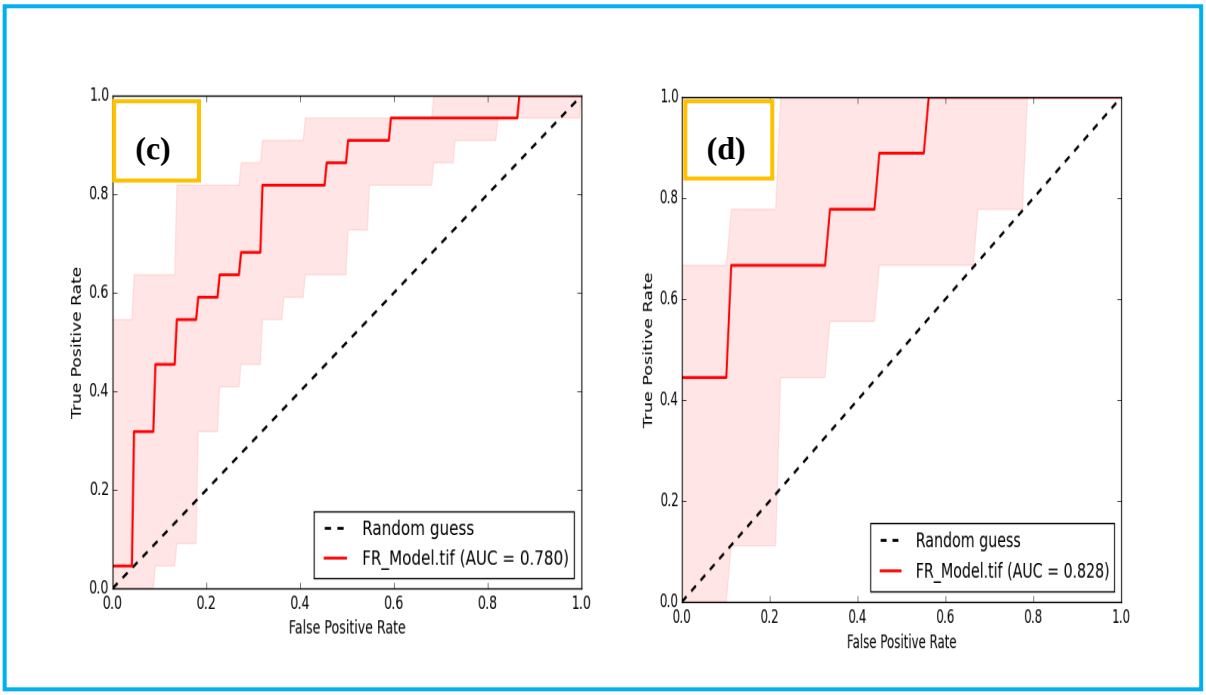

Figure 6.4: Model validation.

AUC values of success rate (a) and prediction rate (b) for the information value model, and success rate (c), and prediction rate (d) for the frequency ratio model.

6.2 Discussion

Landslides are a prevalent geo-environmental issue in Ethiopia, especially in the hilly areas (Bekele Abebe et al., 2010). The study area is situated in the northern Ethiopian plateau, with the majority of the area being sloppy terrain where landslides frequently damage infrastructure, residential structures, and natural landscapes. To mitigate these hazards, it is crucial to identify the contributing factors and delineate the area into different susceptible classes (Anbalagan, 1992). In this study, the information value and frequency ratio models were applied to generate a landslide susceptibility map of the area. The predisposing factors such as slope, aspect, elevation, distance to streams, LULC, and lithology were considered. These factors were selected based on literature and field observations, with varying degrees of importance. The FR and IV results (Table 6.1) reveal that the geomorphological factors such as slope, elevation, and aspect are significant contributors to landslide occurrence, consistent with the study by Lee & Pradhan (2007). Based on the results observed in Table 6.1, it is evident that as the slope angle increases, both the FR and IV values increase, aligning with the findings by Matebie Meten et al. (2015). Although the influence

of topography is more significant in this study, the contribution of other factors is unforgettable. The results also indicate a high correlation between slope materials and landslides, particularly in the weathered and fractured basalt class. The highest FR and IV values for slope and elevation as well as for lithology (weathered and fractured basalt) were observed in the same locations. This indicates that slope and elevation are largely controlled by lithology, where fracture and weathering reduce rock strength, making these areas more prone to landslides (Raghuvanshi et al., 2014). Most past landslides are observed in weathered and fractured basalt units and the analysis result also shows a higher association between fractured and weathered basalts and landslides. This could be due to the combined influences of topography and geology on the landslide incidents. Regarding distance to the stream, Table 6.1 of FR and IV results suggest a high probability of landslide incidents near streams and rivers. The result reveals that the correlation between streams and landslides is significant. Typically, landslides are less common in vegetated areas as compared to barren lands. Through its roots, vegetation can enhance slope stability and soil erosion because the roots uptake more water and bind the soil together, thus reducing the water content in the soil (Löbmann et al., 2020). However, this study found a high incidence of landslides in vegetated areas, likely due to steep slopes and the presence of weathered and fractured basalt. Other factors such as the species and root characteristics, human activities, soil type and properties, slope morphology, and geology also aggravate landslide occurrences in vegetated area (Li & Duan, 2024). In this research, a high proportion of landslide occurrences was observed in the vegetated land class (Table 6.1). This could be associated with slope geometry lithology, root characteristics, soil type, and plat species. Within the vegetated LULC class, the area exhibits steeper slope angles and weathered and fractured basalt units. Steep terrains are inherently highly exposed to landslides. Therefore, vegetation on steep slopes can contribute to landslide occurrences, particularly when the soil become saturated. Vegetation can retain water in the soil, increasing the load on the soil and reducing the stability of the slope.

Different classifier techniques can be applied to divide the area into different susceptibility classes (Lulseged Ayalew et al., 2004). The research region was divided into five (5) susceptibility classes using Jenks natural interval as it is applicable to categorize areas with non-uniform data distribution (Azemeraw Wubalem, 2020). The existing landslide location is unevenly distributed in the research area. Accordingly, the area is classified into 5 susceptible classes; Very high, high, moderate, low, and very low susceptible classes (Fig. 6.3). The very high and high susceptibility

classes are associated with weathered and fractured basalts and steep slopes, while the very low and low susceptibility classes correspond to gentle slopes and colluvial deposits. Although colluvial and alluvial deposits are generally prone to slope failure, they are mainly governed by the topography. The FR model results indicate that 9 km^2 (9%) of the area is covered by very high susceptibility, 11 km^2 (11%) by high susceptibility, 17 km^2 (17%) by moderate susceptibility, 23 km^2 (23%) by low susceptibility, and 40 km^2 (40) by very low susceptibility. Similarly, the IV model shows 18 km^2 (18%) with very susceptibility, 12 km^2 (12%) with high susceptibility, 17 km^2 (17%) with moderate susceptibility, 18 km^2 (18%) with low susceptibility, and 35 km^2 (35) with very low susceptibility.

The AUC for the success and prediction rate served as validation for the results. According to the validation, the FR model showed an AUC of 0.78 for the success rate and 0.828 for the prediction rate, while the IV model showed values of 0.786 and 0.83, respectively. These results demonstrate that both models effectively predict landslide susceptibility mapping in the study area.

CHAPTER VII

CONCLUSION AND RECOMMENDATION

7.1 Conclusion

This study employed information value and frequency ratio models to generate a landslide susceptibility map of the Wuchale area. A total of 31 existing landslides were identified. To understand the underlying causes of these landslides, six key conditioning factors were selected: slope, elevation, aspect, lithology, LULC, and distance to stream. All the parameters were chosen for their relevance to the region's geological and topographical context. Slope has a significant influence on landslide occurrences, followed by elevation, slope material, aspect, LULC, and distance to stream. While, based on the results computed by the information value model, distance to stream has a greater influence on landslides, followed by slope, LULC, aspect, slope material, and elevation.

The study found that the slope (>45^{o}), aspect (north), elevation (2060-2459 m), distance to stream (0-50 m), LULC (vegetated area), and slope material (fractured and weathered basalt) classes have a prominent influence on slope stability.

Using the combined training landslide dataset and each influencing factor, a landslide susceptibility map was generated for both FR and IV models. This map was stratified into five (5) categories: very low, low, moderate, high, and very high susceptibility classes, determined by the Jenks natural breaks classification method considering the landslide susceptibility index ranges.

To validate the accuracy of the landslide susceptibility map, an accurate assessment of the model's ability to classify the area and predict future landslides were conducted. From the total of 31 landslide inventory points, 70% (22 points) were utilized for training, while the remaining 30% (9 points) were served for validation purposes. The model's performance was quantified using the Area under the Receiver Operating Characteristic (ROC) curve, calculated within a GIS environment via ArcSDM tool. The validation outcomes indicated that the frequency ratio model achieved success and prediction rate AUC values of 0.78 and 0.828 respectively, whereas the information value model attained comparable success and prediction rate of 0.786 and 0.83, respectively. These findings affirm the suitability and efficacy of the applied models for landslide susceptibility mapping in the study area.

7.2 Recommendation

Based on the field observations and analysis results of this study, the hilly topography of the study area is predominantly covered with high and very high susceptibility classes, which will pose significant damage to people and infrastructures. Therefore, special attention should be given by the local community and government to implement risk reduction and mitigation measures, such as diversion channels, gabions, or retaining walls, particularly in areas near streams. Additionally, the local community should implement proper land use practices, particularly in Qina Amba site.

Significant impacts were observed in the study area, particularly in Graar Genda, where 174 houses were completely demolished, and 533 people were evacuated from their residences. Therefore, residents, particularly in Graar Genda site should be relocated to stable areas.

The Ambasel Woreda Disaster prevention and preparedness team should record the information about the landslide occurrences.

References

Abbate, E., Bruni, P., & Sagri, M. (2015). Geology of Ethiopia: A Review and Geomorphological Perspectives. In *Landscapes and Landforms of Ethiopia* (pp. 33-64).

Abbate, E., Sagari, M. (1980). Volcanites of Ethiopian and Somali plateaus and major tectonic lines. Atti Convegni Acc Lincei Roma, 47:219-227.

Anbalagan, R. (1992). Landslide hazard evaluation and zonation mapping in mountainous terrain. *Engineering Geology*, *32(4)*, 269-277.

Azemeraw Wubalem. (2020). Modeling of Landslide Susceptibility in a part of Abay Basin, northwestern Ethiopia. *Open Geosciences*, *12*(1), 1440-1467. https://doi.org/10.1515/geo-2020-0206

Beccaluva, L., Bianchini, G., Natali, C., & Siena, F. (2009). Continental Flood Basalts and Mantle Plumes: a Case Study of the Northern Ethiopian Plateau. *Journal of Petrology*, *50*(7), 1377-1403. https://doi.org/10.1093/petrology/egp024

Bekele Abebe, Darmis F., Fubelli, G., Umer, M., & Asfawossen Asrat. (2010). Landslides in the Ethiopian highlands and the Rift margins. *Journal of African Earth Sciences*, *56*, 131-138. https://doi.org/10.1016/j.jafrearsci.2009.06.006

Birhane Girum, Takele Chekol, & Daniel Meshesha. (2023). Petrological and geochemical characteristics of flood and shield basalts from Kesem-Megezez section, northwestern Ethiopian Plateau: Implication for their mantle source variations. *Heliyon*, *9*(6), e17256. https://doi.org/10.1016/j.heliyon.2023.e17256

Chen, L., Guo, Z., Yin, K., Shrestha, D. P., & Jin, S. (2019). The influence of land use and land cover change on landslide susceptibility: a case study in Zhushan Town, Xuan'en County (Hubei, China). *Natural Hazards and Earth System Sciences*, *19*(10), 2207-2228.

Dai, F., & Lee, C. (2001). Terrain-based mapping of landslide susceptibility using a geographical information system: a case study. *Canadian Geotechnical Journal*, *38*(5), 911-923.

Dai, F., Lee, C. F., & Ngai, Y. Y. (2002). Landslide risk assessment and management: an overview. *Engineering Geology*, *64*(1), 65-87.

Das, S., Sarkar, S., & Kanungo, D. P. (2022). A critical review on landslide susceptibility zonation: recent trends, techniques, and practices in Indian Himalaya. *Natural hazards*, *115*(1), 23-72. https://doi.org/10.1007/s11069-022-05554-x

Dawit Asmare. (2023). Application and validation of AHP and FR methods for landslide susceptibility mapping around Choke Mountain, northwestern Ethiopia. *Scientific African*, *19*. https://doi.org/10.1016/j.sciaf.2022.e01470

Dereje Ayalew, Pierre, B., Bernand. M., Laurie, R., Gezahegn Yirgu & Pik, R. (2002). Source, genesis, and timing of giant ignimbrite deposits associated with Ethiopian continental flood basalts. *Geochimica et Cosmochimica Acta*, *66*(8), 1429–1448.

Dereje Ayalew. (2011). The relations between felsic and mafic volcanic rocks in continental flood basalts of Ethiopia: implication for the thermal weakening of the crust. *Geological Society, London, Special Publications*, *357*(1), 253-264. https://doi.org/10.1144/sp357.13

Duncan, W., & Norman, N. (1996). Rock Slope Stability Analysis. *Landslides: investigation and mitigation*, 391-425.

Ebinger, C. J., & Sleep, N. H. (1998). Cenozoic magmatism throughout East Africa resulting from impact of a single plume. *Nature*, *395*(6704), 788-791.

Fall, M., Azzam, R., & Noubactep, C. (2006). A multi-method approach to study the stability of natural slopes and landslide susceptibility mapping. *Engineering Geology*, *82*(4), 241-263.

Food and Agriculture Organization of the United Nations. (2005). "A System of Integrated Agricultural Censuses and Surveys: Volume 1 - World Programme for the Census of Agriculture 2010." Rome, Italy: FAO.

Filagot Mengistu, Suryabhagavan, K. V., Raghuvanshi, T. K., & Lewi, E. (2019). Landslide Hazard Zonation and Slope Instability Assessment using Optical and InSAR Data: A Case Study from Gidole Town and its Surrounding Areas, Southern Ethiopia. *Remote Sensing of Land, 3*(1), 1-14. https://doi.org/10.21523/gcj1.19030101

Gezahegn, Y. (1997). Magma-crust interaction during emplacement of Cenozoic volcanism in Ethiopia: geochemical evidence from Sheno-Magezez area Central Ethiopia. *SINET: Ethiopian Journal of Science, 20*(1), 49-72.

Henriques, C., Zêzere, J. L., & Marques, F. (2015). The role of the lithological setting on the landslide pattern and distribution. *Engineering Geology, 189*, 17-31.

Herold, M., Latham, J. S., Di Gregorio, A., & Schmullius, C. C. (2006). Evolving standards in land cover characterization. *Journal of Land Use Science*, *1*(2-4), 157-168.

Highland, L. M., & Bobrowsky, P. (2008). *The landslide handbook-A guide to understanding landslides*. US Geological Survey.

Hofmann, C., Courtillot, V., Feraud, G., Rochette, P., Gezahegn Yirgu., Ketefo, E., & Pik, R. (1997). Timing of the Ethiopian flood basalt event and implications for plume birth and global change. *Nature*, *389*(6653), 838-841.

https://southwollocommunication.gov.et/News/SinglePost/535.

Kanungo, D. P., Arora M. K., Sarkar S., & Gupta R. P. (2009). Landslide Hazard Zonation in India: A Review. *Journal of South Asia Disaster Studies*, *2*(1), 349-354.

Kaur, H., Gupta, S., & Parkash, S. (2017). Comparative evaluation of various approaches for landslide hazard zoning: a critical review in Indian perspectives. *Spatial Information Research*, *25*(3), 389-398. https://doi.org/10.1007/s41324-017-0105-7

Kazmin, V. (1979). Stratigraphy and correlation of Cenozoic volcanic rocks in Ethiopia. *Reports of Ethiopian Institute of Geological Survey*, *106*, 1-26.

Kieffer, B., Arndt, N., Lapierre, H., Bastien, F., Bosch, D., Pecher, A., Gezahegn Yirgu, Dereje Ayalew, Weis, D., Jerram, D. A., Keller, F., & Meugniot, C. (2004). Flood and Shield Basalts from Ethiopia: Magmas from the African Superswell. *Journal of Petrology*, *45*(4), 793-834. https://doi.org/10.1093/petrology/egg112

Kifle Woldearegay. (2013). Review of the occurrences and influencing factors of landslides in the highlands of Ethiopia: With implications for infrastructural development *Momona Ethiopian Journal of Science*, *5*(1), 3-31.

Lee, S., & Pradhan, B. (2007). Landslide hazard mapping at Selangor, Malaysia using frequency ratio and logistic regression models. *Landslides*, *4*(1), 33-41.

Leulalem Shano, Raghuvanshi, T. K., & Matebie Meten. (2021). Landslide susceptibility mapping using frequency ratio model: the case of Gamo highland, South Ethiopia. *Arabian Journal of Geosciences*, *14*(7). https://doi.org/10.1007/s12517-021-06995-7

Leulalem Shano, Raghuvanshi, T. k., & Matebie Meten. (2020). Landslide susceptibility evaluation and hazard zonation techniques–a review. *Geoenvironmental Disasters*, *7*(1), 1-19. https://doi.org/10.1186/s40677-020-00152-0

Li, B., Wang, N., Chen, J., & Ji, J. (2021). GIS-Based Landslide Susceptibility Mapping Using Information, Frequency Ratio, and Artificial Neural Network Methods in Qinghai Province, Northwestern China. *Advances in Civil Engineering*, *2021*, 1-14.

Li, Y., & Duan, W. (2024). Decoding vegetation's role in landslide susceptibility mapping: An integrated review of techniques and future directions. *Biogeotechnics, 2*(1).

Li, Y., Wang, X., & Mao, H. (2020). Influence of human activity on landslide susceptibility development in the Three Gorges area. *Natural hazards, 104*, 2115-2151.

Löbmann, M. T., Geitner, C., Wellstein, C., & Zerbe, S. (2020). The influence of herbaceous vegetation on slope stability – A review. *Earth-Science Reviews, 209*.

Lulseged Ayalew, Yamagishi, H., & Ugawa, N. (2004). Landslide susceptibility mapping using GIS-based weighted linear combination, the case in Tsugawa area of Agano River, Niigata Prefecture, Japan. *Landslides, 1*(1), 73-81. https://doi.org/10.1007/s10346-003-0006-9

Mandal, B., & Mandal, S. (2017). Landslide susceptibility mapping using modified information value model in the Lish river basin of Darjiling Himalaya. *Spatial Information Research, 25*(2), 205-218. https://doi.org/10.1007/s41324-017-0096-4

Matebie Meten, Bhandary, N. P., & Yatabe, R. (2015). GIS-based frequency ratio and logistic regression modelling for landslide susceptibility mapping of Debre Sina area in central Ethiopia. *Journal of Mountain Science, 12*, 1355-1372. https://doi.org/10.1007/s1162

Mengesha Tefera, Tadiwos Chernet, & Workineh Haro. (1996). *Explanation of the geological map of Ethiopia*. Geological Survey of Ethiopia.

Mohr, P., & Zanettin, B. (1988). The Ethiopian Flood Basalt Province. *ContinenJal Flood Basalts*, 63-110.

Nikolic, T. (2015). Direct and Indirect Impact of Landslide on Environment. In *Engineering Geology for Society and Territory* (Vol. 5, pp. 1237-1241). Springer International Publishing. https://doi.org/10.1007/978-3-319-09048-1_236

Pacheco Quevedo, R., Velastegui-Montoya, A., Montalván-Burbano, N., Morante-Carballo, F., Korup, O., & Daleles Rennó, C. (2023). Land use and land cover as a conditioning factor in landslide susceptibility: a literature review. *Landslides*, *20*(5), 967-982.

Picarelli, L., Leroueil, S., Olivares, L., Pagano, L., Tommasi, P., & Urciuoli, G. (2012). Groundwater in slopes. In John J. Clague & D. Stead (Eds.), *Landslides* (pp. 235-251). Cambridge University Press. https://doi.org/10.1017/cbo9780511740367.021

Pik, R., Deniel, C., Coulon, C., Gezahegn Yirgu & Marty, B. (1999). Isotopic and trace element signatures of Ethiopian flood basalts: evidence for plume lithosphere interactions. *Geochimica et Cosmochimica Acta*, *63*(15), 2263-2279.

Raghuvanshi, T. K., Jemal Ibrahim & Dereje Ayalew (2014). Slope stability susceptibility evaluation parameter (SSEP) rating scheme–an approach for landslide hazard zonation. *Journal of African Earth Sciences*, *99*, 595-612.

Remondo, J., González, A., De Terán, J. R. D., Cendrero, A., Fabbri, A., & Chung, C. J. F. (2003). Validation of landslide susceptibility maps; examples and applications from a case study in Northern Spain. *Natural hazards*, *30*, 437-449.

Sarkar, S., & Kanungo, D. (2004). An integrated approach for landslide susceptibility mapping using remote sensing and GIS. *Photogrammetric Engineering & Remote Sensing*, *70(5)*, 617-625.

Sarkar, S., Roy, A. K., & Martha, T. R. (2013). Landslide susceptibility assessment using information value method in parts of the Darjeeling Himalayas. *Journal of the Geological Society of India*, *82*, 351-362.

Sendu Demessie & Raghuvanshi, T. K. (2019). Landslide hazard evaluation and zonation in Dilbe Town and its surrounding areas, Northwestern Central Ethiopia – A GIS based grid overlay statistical approach. *Journal of Geomatics*, *13*(1), 79-92.

Singhroy V., (1995). SAR integrated techniques for geohazard assessment. *Advances in Space Research*, *15(11)*, 67-78.

Sun, L., Grasselli, G., Liu, Q., Tang, X., & Abdelaziz, A. (2022). The role of discontinuities in rock slope stability: Insights from a combined finite-discrete element simulation. *Computers and Geotechnics*, *147*. https://doi.org/10.1016/j.compgeo.2022.104788

Tadele Melese, Tatek Belay & Azene Andemo. (2022). Application of analytical hierarchal process, frequency ratio, and Shannon entropy approaches for landslide susceptibility mapping using geospatial technology: The case of Dejen district, Ethiopia. *Arabian Journal of Geosciences*, *15*(5). https://doi.org/10.1007/s12517-022-09672-5

Tesfaye Demissie, Genet Yohannes, Abraham Mammo, Yibeltal Tesfaye, Yonas Teshome, Getachew Burusa, Mohammed Edris & Meran Wenduante. (2010). *Geology geochemistry and gravity survey of the Dessie area* [Unpublished Report]. Geological Survey of Ethiopia.

Thapa, D., & Bhandari, B. P. (2019). GIS-Based Frequency Ratio Method for Identification of Potential Landslide Susceptible Area in the Siwalik Zone of Chatara-Barahakshetra Section, Nepal. *Open Journal of Geology*, *09*(12), 873-896.

Tilahun Hamza & Raghuvanshi, T. K. (2017). GIS-based landslide hazard evaluation and zonation–A case from Jeldu District, Central Ethiopia. *Journal of King Saud University-Science*, *29*(2), 151-165. https://doi.org/10.1016/j.jksus.2016.05.002

Tyagi, A., Kamal Tiwari, R., & James, N. (2022). A review on spatial, temporal and magnitude prediction of landslide hazard. *Journal of Asian Earth Sciences: X, 7*.

Ukstins, I. A., Renne, P. R., Wolfenden, E., Baker, J., Dereje Ayalew., & Menzies, M. (2002). Matching conjugate volcanic rifted margins: 40Ar/39Ar chrono-stratigraphy of pre- and syn-rift bimodal £ood volcanism in Ethiopia and Yemen. *Earth and Planetary Science Letters, 198* 289-306.

Valagussa, A., Marc, O., Frattini, P., & Crosta, G. B. (2019). Seismic and geological controls on earthquake-induced landslide size. *Earth and Planetary Science Letters*, *506*, 268-281.

Van Westen, C. J. (1993). Remote sensing and geographic information systems for geologic hazard mitigation. *ITC journal*, 393-393.

Van Westen, C. J., Rengers, N., Terlien, M., & Soeters, R. (1997). Prediction of the occurrence of slope instability phenomena through GIS-based hazard zonation. *Geologische Rundschau*, *86*(2), 404-414.

Varnes, D. J. (1978). Slope movement types and processes. Special Report *176*, 11-33.

Varnes, D. J. (1984). *Landslide hazard zonation: a review of principles and practice*.

Yesilnacar, E., & Topal, T. (2005). Landslide susceptibility mapping: A comparison of logistic regression and neural networks methods in a medium scale study, Hendek region (Turkey). *Engineering Geology*, *79*(3-4), 251-266. https://doi.org/10.1016/j.enggeo.2005.02.002

Yin, K. J., & Yan, T. Z. (1988). Statistical prediction model for slope instability of metamorphosed rocks. Proceedings of the 5th International Symposium on Landslides.

Zanettin, B., EJ, V., Nicoletti, M., & EM, P. (1980). Correlation among Ethiopian volcanic formation with special reference to the chronological and stratigraphical problems of the trap series.

Zhao, Y., Li, Y., Zhang, L., & Wang, Q. (2016). Groundwater level prediction of landslide based on classification and regression tree. *Geodesy and Geodynamics, 7*(5), 348-355.

Appendix I: Ambasel woreda agricultural office report

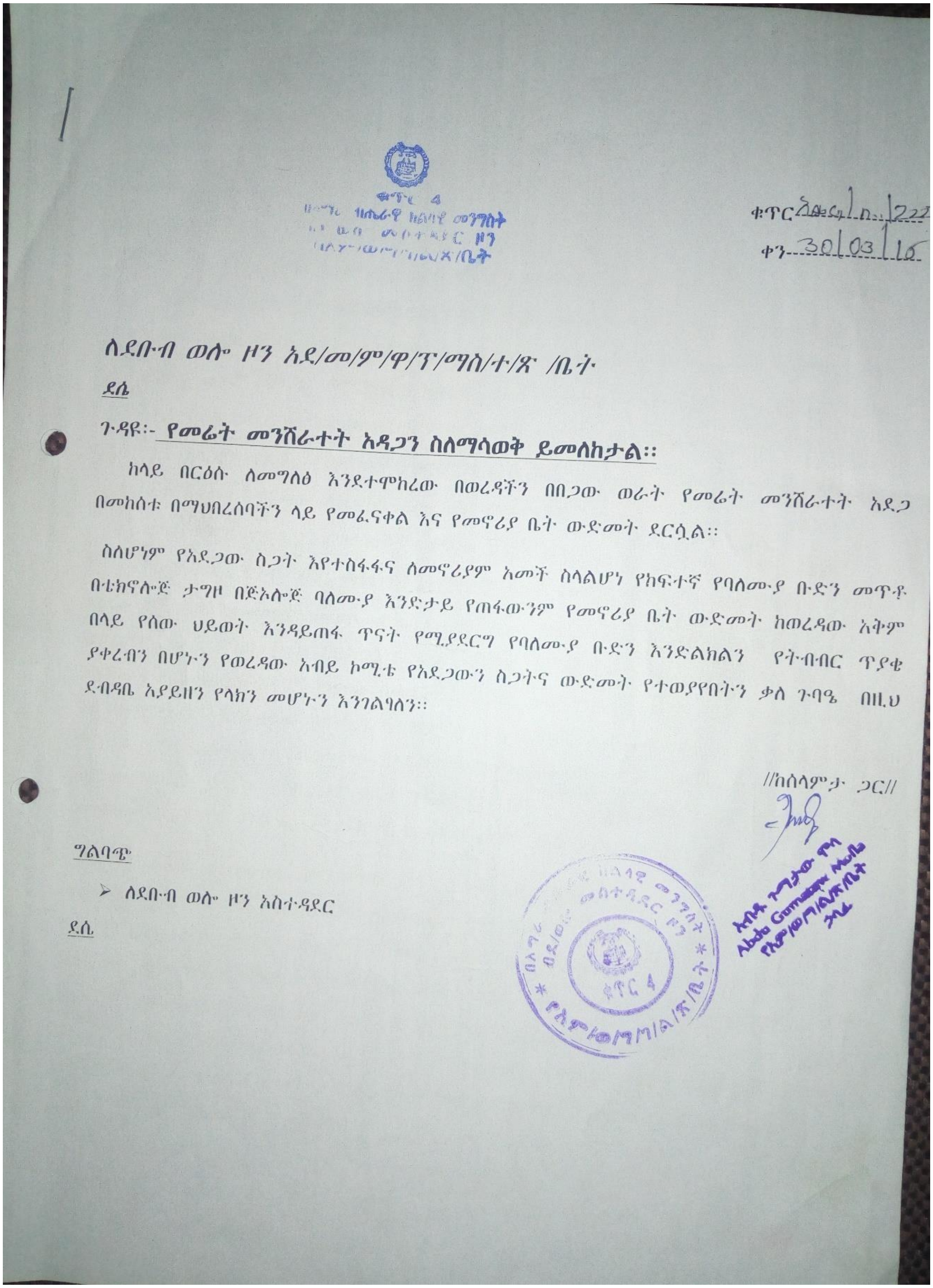

ቀጥር
ቀን 30/03/16

ለደቡብ ወሎ ዞን አደ/መ/ም/ዋ/ፕ/ማስ/ተ/ጽ /ቤት

ደሴ

ጉዳዩ:- የመሬት መንሸራተት አዳጋን ስለማሳወቅ ይመለከታል፡፡

ከላይ በርዕሱ ለመግለፅ እንደተሞከረው በወረዳችን በበጋው ወራት የመሬት መንሸራተት አደጋ በመከሰቱ በማህበረሰባችን ላይ የመፈናቀል እና የመኖሪያ ቤት ውድመት ደርሷል፡፡

ስለሆነም የአደጋው ስጋት እየተስፋፋና ለመኖሪያም አመች ስላልሆነ የከፍተኛ የባለሙያ ቡድን መጥቶ በቴክኖሎጅ ታግዞ በጅኦሎጅ ባለሙያ እንድታይ የጠፋውንም የመኖሪያ ቤት ውድመት ከወረዳው አቅም በላይ የሰው ህይወት እንዳይጠፋ ጥናት የሚያደርግ የባለሙያ ቡድን እንድልክልን የትብብር ጥያቄ ያቀረብን በሆኑን የወረዳው አብይ ኮሚቴ የአደጋውን ስጋትና ውድመት የተወያየበትን ቃለ ጉባዔ በዚህ ደብዳቤ አያይዘን የላክን መሆኑን እንገልፃለን፡፡

//ከሰላምታ ጋር//

ግልባጭ

- ለደቡብ ወሎ ዞን አስተዳደር

ደሴ

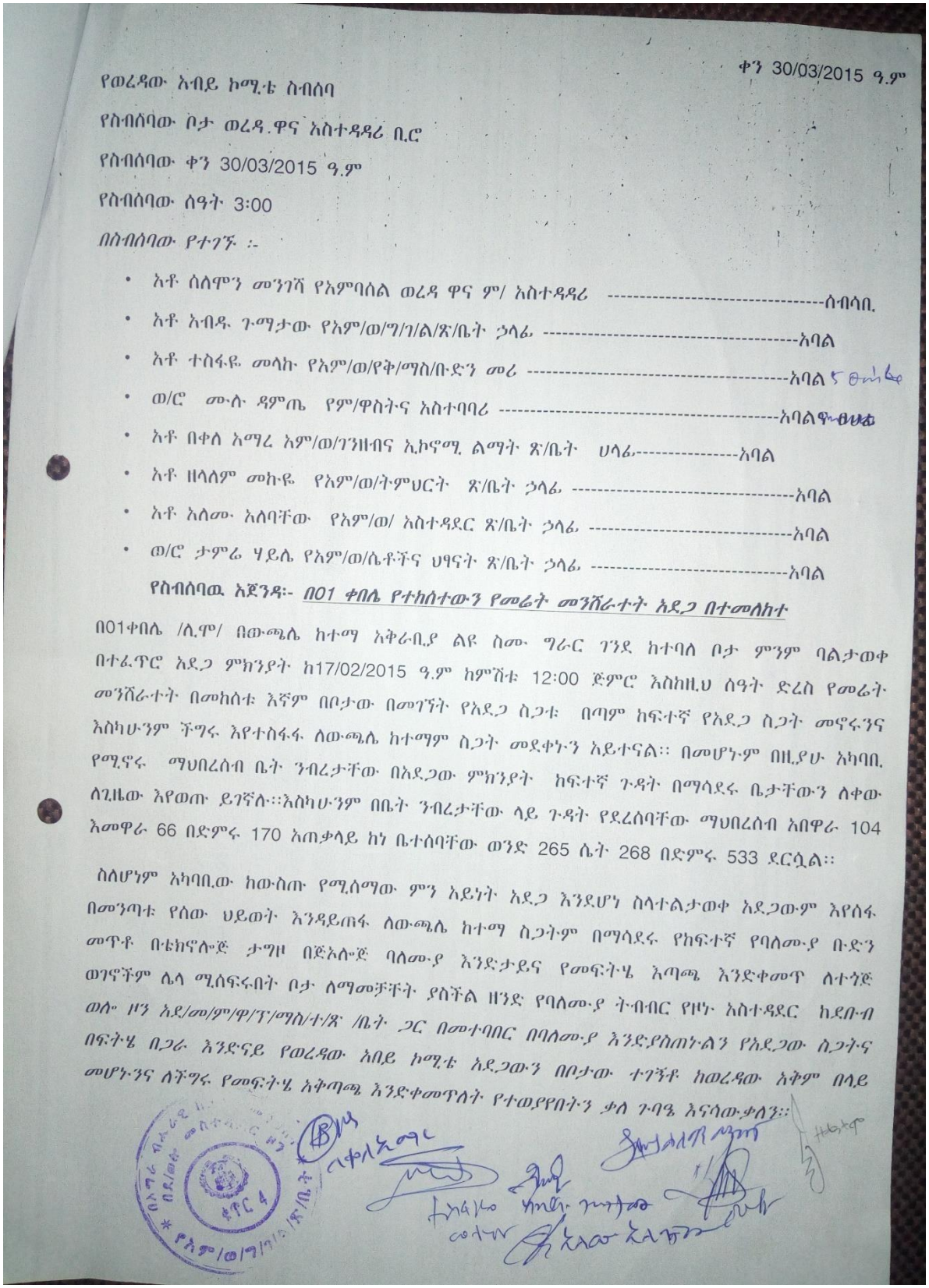

ቀን 30/03/2015 ዓ.ም

የወረዳው አብይ ኮሚቴ ስብሰባ

የስብሰባው ቦታ ወረዳ.ዋና አስተዳዳሪ ቢ.ሮ

የስብሰባው ቀን 30/03/2015 ዓ.ም

የስብሰባው ሰዓት 3:00

በስብሰባው የተገኙ ፡-

- አቶ ሰለሞን መንገሻ የአምባሰል ወረዳ ዋና ም/ አስተዳዳሪ ----------ሰብሳቢ.
- አቶ አብዱ ጉማታው የአም/ወ/ግ/ገ/ል/ጽ/ቤት ኃላፊ ----------አባል
- አቶ ተስፋዬ መላኩ የአም/ወ/የቅ/ማስ/ቡድን መሪ ----------አባል
- ወ/ሮ ሙሉ ዳምጤ የም/ዋስትና አስተባባሪ ----------አባል
- አቶ በቀለ አማረ አም/ወ/ገንዘብና ኢኮኖሚ ልማት ጽ/ቤት ሀላፊ----------አባል
- አቶ ዘላለም መኩዬ የአም/ወ/ትምህርት ጽ/ቤት ኃላፊ ----------አባል
- አቶ አለሙ አለባቸው የአም/ወ/ አስተዳደር ጽ/ቤት ኃላፊ ----------አባል
- ወ/ሮ ታምሬ ሃይሌ የአም/ወ/ሴቶችና ህፃናት ጽ/ቤት ኃላፊ ----------አባል

የስብሰባዉ አጀንዳ፡- ***በ01 ቀበሌ የተከሰተውን የመሬት መንሸራተት አደጋ በተመለከተ***

በ01ቀበሌ /ሊሞ/ በውጫሌ ከተማ አቅራቢያ ልዩ ስሙ ግራር ገንደ ከተባለ ቦታ ምንም ባልታወቀ በተፈጥሮ አደጋ ምክንያት ከ17/02/2015 ዓ.ም ከምሽቱ 12:00 ጅምሮ እስከዚህ ሰዓት ድረስ የመሬት መንሸራተት በመከሰቱ እኛም በቦታው በመገኘት የአደጋ ስጋቱ በጣም ከፍተኛ የአደጋ ስጋት መኖሩንና እስካሁንም ችግሩ እየተስፋፋ ለውጫሌ ከተማም ስጋት መደቀኑን አይተናል፡፡ በመሆኑም በዚያሁ አካባቢ የሚኖሩ ማህበረሰብ ቤት ንብረታቸው በአደጋው ምክንያት ከፍተኛ ጉዳት በማሳደሩ ቤታቸውን ለቀው ለጊዜው እየወጡ ይገኛሉ፡፡እስካሁንም በቤት ንብረታቸው ላይ ጉዳት የደረሰባቸው ማህበረሰብ አበዋራ 104 እመዋራ 66 በድምሩ 170 አጠቃላይ ከነ ቤተሰባቸው ወንድ 265 ሴት 268 በድምሩ 533 ደርሷል፡፡

ስለሆነም አካባቢው ከውስጡ የሚሰማው ምን አይነት አደጋ እንደሆነ ስላተልታወቀ አደጋውም እየሰፋ በመንጣቱ የሰው ህይወት እንዳይጠፋ ለውጫሌ ከተማ ስጋትም በማሳደሩ የከፍተኛ የባለሙያ ቡድን መጥቶ በቴክኖሎጅ ታግዞ በጅኦሎጅ ባለሙያ እንድታይና የመፍትሄ እጣጫ እንድቀመጥ ለተጎጅ ወገኖችም ሌላ ሚሰፍሩበት ቦታ ለማመቻቸት ያስችል ዘንድ የባለሙያ ትብብር የዞኑ አስተዳደር ከደቡብ ወሎ ዞን አደ/መ/ም/ዋ/ፕ/ማስ/ተ/ጽ /ቤት ጋር በመተባበር በባለሙያ እንድያስጠኑልን የአደጋው ስጋትና በፍትሄ በጋራ እንድናይ የወረዳው አበይ ኮሚቴ አደጋውን በቦታው ተገኝቶ ከወረዳው አቅም በላይ መሆኑንና ለችግሩ የመፍትሄ አቅጣጫ እንድቀመጥለት የተወያየበትን ቃለ ጉባዔ እናሳውቃለን፡፡

Appendix II: Precipitation data of Wuchale area

Wuchale station

Year	Jan	Feb	Mar	Apr	May	Jun	Jul	Aug	Sep	Oct	Nov	Dec	Annual
2000	0	0	12.8	87.5	129.8	14	344.6	330.3	108.8	77.6	60.9	175.1	1341.4
2001	21.8	43.7	200.2	13.8	43.4	53.7	356.3	347.6	235.9	27.7	2.3	1.2	1347.6
2002	137.8	9.5	50	85.5	8.5	1	301	272.6	107.4	16.5	0	104.7	1094.5
2003	136.1	35.2	44.8	168.6	6.9	59.4	199.1	307.9	144.1	1.7	23.3	51.9	1179
2004	6.3	70.5	77.4	188.2	23	45.6	199	270.6	86.9	51.8	74.3	76.9	1170.5
2005	24.4	0	86.4	134.2	134.5	24.7	328.9	313.9	44.5	20.9	30.4	0	1142.8
2006	0	2.9	210.6	155.3	42.3	5.8	193	296.7	121.1	50.6	17.6	0	1095.9
2007	53.1	60.5	58.7	106.5	7.9	45.8	440.8	283	143.4	28.8	3	0	1231.5
2008	13.2	1.3	0	22.8	47.2	35.2	224.3	252.2	162.6	96.1	82	0	936.9
2009	29.4	21.6	36.7	30	16.5	33.9	253.7	268.6	30.5	22.7	47.7	70.9	862.2
2010	1.5	21.8	97.7	120.8	90.5	2.2	485.7	717.1	65.3	10.6	13.2	17.2	1643.6
2011	27.6	5	85	86.1	232.3	20	214	300.5	32.6	17	180.3	0	1200.4
2012	0	0	87	193.5	95.6	56.6	463.4	361.6	78.7	41.8	0	6	1384.2
2013	78.8	12	44.9	65.9	19.3	12.1	375.1	317.5	72	79	4	3.4	1084
2014	8.9	25.8	61.5	90.8	134.1	6.2	254.2	356.5	186.6	91	16.7	0	1232.3
2015	55.5	5.4	65.4	0	276.1	0	0	0	0	0	0	0	402.4

Mersa Station

Year	Jan	Feb	Mar	Apr	May	Jun	Jul	Aug	Sep	Oct	Nov	Dec	Total
2000	0	0	0	57.5	49.7	12.2	258.2	386.1	106.3	116.2	36.5	38.7	1061.4
2001	2	18	206	3	80.5	24.8	303.3	0	124.5	25	2.4	5.5	795
2002	129.6	0	40.2	59.8	5.9	3.5	227.8	253.7	87.6	0	0	104.7	912.8
2003	43.4	18.1	43.6	167.8	0	40	121.8	284.9	124.2	1.8	8.2	45	898.8
2004	56.7	27.9	68.7	152.2	2.7	17	190	155.5	0.6	36.5	68.4	19.9	796.1
2005	0	0	54.5	84.3	143.2	27.8	214.1	322	32.6	18	38	0	934.5
2006	4.3	1.6	279.5	137.1	41.2	24.2	158.7	327.8	127.1	89.3	12.7	11.1	1214.6
2007	18	68.5	40.8	97.2	44.1	33.1	336.2	256.3	98.8	30.6	4.5	0	1028.1
2008	43.2	0	0	42.8	33.7	22.6	200.8	221.1	115.3	40.1	43.4	0	763
2009	35.1	6.4	52.7	137.6	3.2	9.5	233.8	268.5	1.6	28.8	3.8	127.8	908.8
2010	0	49.8	75.4	75.7	148.6	5.2	264.4	546.4	65.8	6.9	18.1	13.4	1269.7
2011	7.9	0	112.2	44	130.3	0	116.8	243.6	37.9	13.1	122.7	0	828.5
2012	0	0	75.5	177.8	56.3	61.2	342.7	265	77.9	33.7	0	0	1090.1
2013	141.2	2.5	67.7	73	6.4	9.3	290.4	230	43.5	54.2	0.4	5.1	923.7
2014	2.3	28.3	81.3	116.8	138.7	1.6	138.3	241.3	167.1	10.7	28	0	954.4
2015	21.9	0	21.5	0	173.3	10.3	22.9	0	0	0	0	0	249.9

2017	0	0	0	0	0	0	256.9	552.8	136.8	47.4	9.9	0	1003.8
2018	27.3	0	48.6	225.1	8.7	96	239.8	453.4	77.6	66.5	108.2	1.6	1352.8
2019	0	65.1	81.6	0	0	54.5	91	100.8	167.2	0	0	0	560.2
2020	52.2	17.5	73.7	0	29.6	42.4	281.1	0	91.8	9.7	49.9	0	647.9
2021	2.6	16.4	0	43.2	95.6	0	343	0	0	0	0	0	500.8
2022	4.9	0	59.7	55.2	5.6	47.2	277.4	301	104.2	0	0	0	855.2
2023	0	29.1	238.1	154.9	116.4	60.6	197.6	226.9	33.2	25.2	0	0	1082
Average	**25.76**	**15.18**	**74.83**	**82.82**	**57.11**	**26.21**	**222.04**	**245.09**	**79.2**	**28.42**	**24.13**	**16.20**	**897.04**